AD-A072 043 MATHEMATICAL SCIENCES NORTHWEST INC BELLEVUE WASH F/G 20/5
ELECTRONIC STATE LASERS BY STABILIZED ELECTRIC DISCHARGES.(U)
APR 75 C H FISHER, S R BYRON N00014-74-C-0366
UNCLASSIFIED MSNW-75-125-1 NL

| OF |
AD A072043

END
DATE FILMED
9-79
DDC

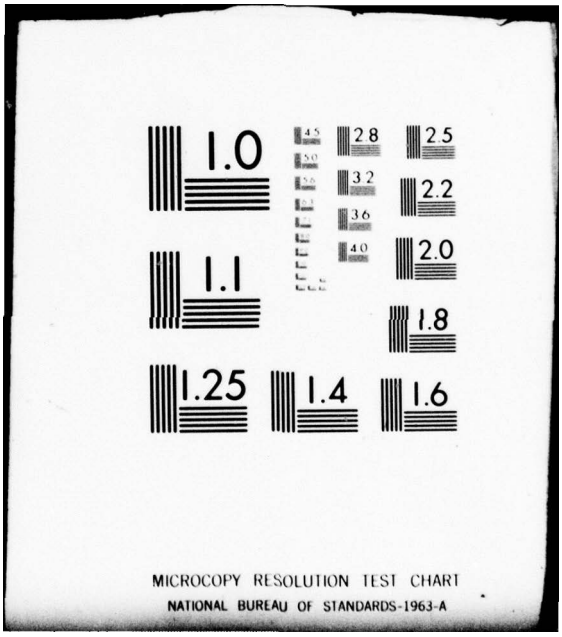
1.0
1.1
1.25
1.4
1.6
1.8
2.0
2.2
2.5
2.8
3.2
3.6
4.0
MICROCOPY RESOLUTION TEST CHART
NATIONAL BUREAU OF STANDARDS-1963-A

ELECTRONIC STATE LASERS BY STABILIZED ELECTRIC DISCHARGES

Final Report
Covering Work Performed During the Period
1 March 1974 through 31 October 1974

by

Charles H. Fisher and Stanley R. Byron

MATHEMATICAL SCIENCES NORTHWEST, INC.
P.O. Box 1887
Bellevue, Washington 98009

April 1975

Contract No. N00014-74-C-0366

Sponsored by

Office of Naval Research
Washington, D. C.

Monitored by

Naval Research Laboratory
Washington, D. C.

AD A072043

DDC ACCESSION NUMBER

II

LEVEL

DATA SHEET

PHOTOGRAPH

THIS SHEET

I

INVENTORY

MSNW Rpt. No. 75-125-1

DOCUMENT IDENTIFICATION

DISTRIBUTION STATEMENT A

Approved for public release;
Distribution Unlimited

DISTRIBUTION STATEMENT

Accession For

NTIS GRA&I

DDC TAB

Unannounced

Justification

By

Distribution/

Availability Codes

Dist	Avail and/or special
A	

DISTRIBUTION STAMP

DDC

RECEIVED

JUL 31 1979

D

DATE ACCESSIONED

79 07 26 081

DATE RECEIVED IN DDC

PHOTOGRAPH THIS COPY

UNCLASSIFIED

SECURITY CLASSIFICATION OF THIS PAGE (When Data Entered)

REPORT DOCUMENTATION PAGE		READ INSTRUCTIONS BEFORE COMPLETING FORM
1. REPORT NUMBER 75-125-1	2. GOVT ACCESSION NO.	3. RECIPIENT'S CATALOG NUMBER
4. TITLE (and Subtitle) Electronic State Lasers by Stabilized Electric Discharges		5. TYPE OF REPORT & PERIOD COVERED Final Report 6. PERFORMING ORG. REPORT NUMBER 75-125-1
7. AUTHOR(s) Charles H. Fisher and Stanley R. Byron		8. CONTRACT OR GRANT NUMBER(s) N00014-74-C-0366
9. PERFORMING ORGANIZATION NAME AND ADDRESS Mathematical Sciences Northwest, Inc. P.O. Box 1887 Bellevue, Washington 98009		10. PROGRAM ELEMENT, PROJECT, TASK AREA & WORK UNIT NUMBERS
11. CONTROLLING OFFICE NAME AND ADDRESS Office of Naval Research Department of the Navy Arlington, Va. 22217		12. REPORT DATE April 1975 13. NUMBER OF PAGES 58
14. MONITORING AGENCY NAME & ADDRESS (if different from Controlling Office) Naval Research Laboratory 4555 Overlook Avenue, SW Washington, DC 20375 code 5540		15. SECURITY CLASS. (of this report) Unclassified 15a. DECLASSIFICATION/DOWNGRADING SCHEDULE

16. DISTRIBUTION STATEMENT (of this Report)

APPROVED FOR PUBLIC RELEASE
DISTRIBUTION UNLIMITED

17. DISTRIBUTION STATEMENT (of the abstract entered in Block 20, if different from Report)

18. SUPPLEMENTARY NOTES

19. KEY WORDS (Continue on reverse side if necessary and identify by block number)

Electronic state lasers
Electron beam
Molecular excitation
Nitrogen
Carbon monoxide
Collisional lasers

20. ABSTRACT (Continue on reverse side if necessary and identify by block number)

This report describes studies aimed at achieving long pulse laser emission in the near infrared, visible or ultraviolet region using electron-beam-stabilized electric discharge excitation of molecular electronic states. A model for long pulse visible laser emission from electronically excited states is described which involves rapid collisional quenching of the vibrational energy of the electronic states. The production and quenching of specific vibrational levels of excited electronic states of N_2 and CO molecules have been

DD FORM 1 JAN 73 1473 EDITION OF 1 NOV 65 IS OBSOLETE

UNCLASSIFIED

SECURITY CLASSIFICATION OF THIS PAGE (When Data Entered)

20. Abstract (continued)

studied by observing the fluorescence from gas mixtures excited by an electric discharge. The excitation efficiency for the $N_2(A^3\Sigma_u^+)$ state was determined by absolute population measurements of the v = 0 and v = 1 vibrational levels using a nitrogen (B → A) probe laser technique. The measured decay rate of the $N_2(A^3\Sigma_u^+)$ state by self-collisions was 3×10^{-9} cm^3/molecule-sec. Laser cavity tests were carried out for both N_2 and CO gas mixtures for a variety of conditions. Short pulse laser action was observed in the N_2 first positive system at 1.05 and 0.888 μm using e-beam-stabilized electric discharge excitation.

TABLE OF CONTENTS

LIST OF TABLES

LIST OF FIGURES

SECTION I

INTRODUCTION

A unique laser concept has been established at Mathematical Sciences Northwest, Inc. (MSNW) which offers excellent prospects for developing high efficiency, high energy density, visible gas lasers. The basis for this laser concept evolved during a previous program at MSNW under an ARPA-ONR contract (Ref. 1) and has been examined more quantitatively during the program reported here. The approach borrows three principles that have been well established in high power infrared laser development and applies these to visible electronic state lasers.

The first principle is the use of electron-beam-stabilized electric discharge excitation which has proved very efficient in IR lasers. The second principle is the use of preferential collisional processes to provide a two-temperature system, in this case a high temperature among electronic states and a low vibrational temperature within each electronic state. The third principle is to recycle the laser molecule many times during the laser pulse, thereby using the gas to its full (thermal) limit; electron impact pumping of the upper laser level and rapid VV and/or VT collisional quenching of the (vibrationally excited) lower laser level accomplish the recycling process.

Three key elements must be combined in order to make this concept a reality. First, a stable pulsed discharge is required which can provide a high rate of electronic excitation, a low rate of vibrational excitation, and sufficient time duration without arc formation. Second,

molecular laser systems must be found which exhibit an allowed visible transition between electronic states for which the potential curve minima are displaced, yielding a high Franck-Condon factor for transitions from the low vibrational levels of the upper state to high vibrational levels of the lower state. This is shown schematically in Figure 1. Third, for candidate laser molecules, collisional processes must be found that provide more rapid quenching of the vibrational levels of the lower state than either the radiative decay or the collisional decay of the upper state.

In searching for candidate laser molecules, attention was directed initially to molecules which have already produced visible laser output in short pulse electric discharges, such as $N_2(C^3\Pi_u \rightarrow B^3\Pi_g)$ and $CO(B^1\Sigma^+ \rightarrow A^1\Pi)$. However, these molecules do not completely fulfill the prescription outlined above; the minima in the potential curves are not markedly shifted, the electronic states involved in laser emission are not among the lowest electronic states of these molecules, and both N_2 and CO have large cross sections for vibrational excitation by electron impact. Nevertheless, if preferential collisional quenching of the vibrational energy within each electronic state can be achieved in these molecules, this will provide the initial foundation for long pulse visible electronic state electric discharge lasers.

Initial experiments at MSNW were directed toward the study of N_2 and CO visible electronic state emission in electric discharges stabilized by a moderate current density (~ 50 ma/cm^2) electron beam. Qualitative studies of kinetic mechanisms and discharge stability were carried out.

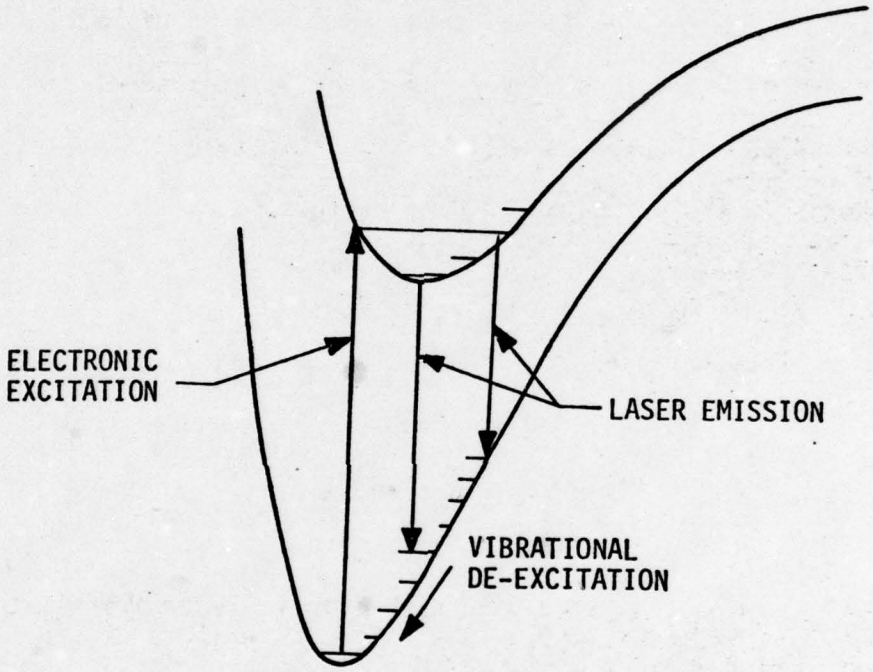

Figure 1. Collision Dominated Visible Electronic State Laser Concept

These results are reported in Reference 1. The work reported here is a direct extension of the concepts developed in the previous program, and some of the studies were carried out in parallel.

The effort under this program has been directed towards optimizing the efficiency of excitation of specific electronic states by an electric discharge. This has involved the study of the production and quenching of vibrational levels of specific excited electronic states of N_2 and CO molecules as well as a quantitative determination of their population. The principal results of this study are summarized here briefly.

1. Fluorescence from electric discharges in Ar+N_2 and He+N_2 mixtures showed evidence of considerable vibrational excitation in the $N_2(C)$ and $N_2(B)$ states. Considerably less vibrational excitation has been observed at other laboratories that have used high energy electron beam excitation.

2. Absolute population measurements of the v = 0 and 1 levels of the $N_2(A^3\Sigma_u^+)$ state as a function of time during and after the electric discharge were made using an $N_2(B\rightarrow A)$ probe laser technique. The peak population occurred near the end of the discharge pulse and was approximately 10^{14} molecules/cm^3. From the decay of the $N_2(A)$ state population after the discharge was terminated, the rate coefficient for the deactivation of the A state by self collisions was found to be roughly 3×10^{-9}cm^3/molecule-sec.

From the measured peak population of the $N_2(A)$ state, the fraction of electric discharge energy that appeared as $N_2(A)$ state molecules was calculated to be approximately 0.1 percent.

3. An absorption scheme utilizing a narrow bandwidth dye laser to measure the population of the lowest vibrational levels of the CO($A'\Pi$) state was devised and was partially developed during this program.

4. Laser cavity tests were carried out for both N_2 and CO with two different electric discharge power supplies. Laser action was observed in the N_2 first position system at 1.05 and 0.888 μm when a high voltage, fast rising electric discharge pulse was employed.

In Section II, a detailed description is given of the kinetic mechanism for long pulse visible laser emission which involves rapid collisional quenching of the vibrational levels of the electronic states. These ideas were evaluated experimentally for electron beam stabilized electric discharge excitation by employing fluorescence emission studies (Section III), probe laser absorption measurements (Section IV), and laser cavity tests (Section V). Conclusions and recommendations based on these results are given in Section VI.

SECTION II

ELECTRONIC STATE KINETIC PROCESSES

In developing a more quantitative understanding of the general principles on which visible, collisional, electronic state lasers will be based, some of the kinetic requirements and restrictions are noted here. To achieve a significant low signal optical gain (0.1 cm^{-1}) in the visible (about 5000 Å), using a diatomic molecule such as N_2, the upper laser level electronic state population must exceed the lower level population by about 10^{13} cm^{-3}, assuming Doppler broadening and a 10^{-7} sec radiative lifetime for the lasing transition. The dependence of the required population on lifetime is shown as the lower curve in Figure 2. An upper bound on the abscissa is shown for this curve, above which the collisional self-destruction loss process exceeds spontaneous emission as a decay mechanism for the upper laser level (assuming a rate constant of 10^{-9} cm^3/ sec). Thus, to avoid self-quenching losses, the radiative lifetime of the laser transition must be less than about 3 μsec.

Assuming a 6 eV excitation energy, the population of the radiating state requires an energy input rate of at least 100 watts/cm^3 (assuming no collisional decay of the upper electronic state). An excitation rate of this magnitude is quite readily achieved in e-beam stabilized electric discharges (e.g., 1 percent efficiency at discharge conditions of 10 amps/cm^2 and 10^3 V/cm).

The population inversion mechanism being considered here involves the simultaneous production of a high molecular electronic temperature

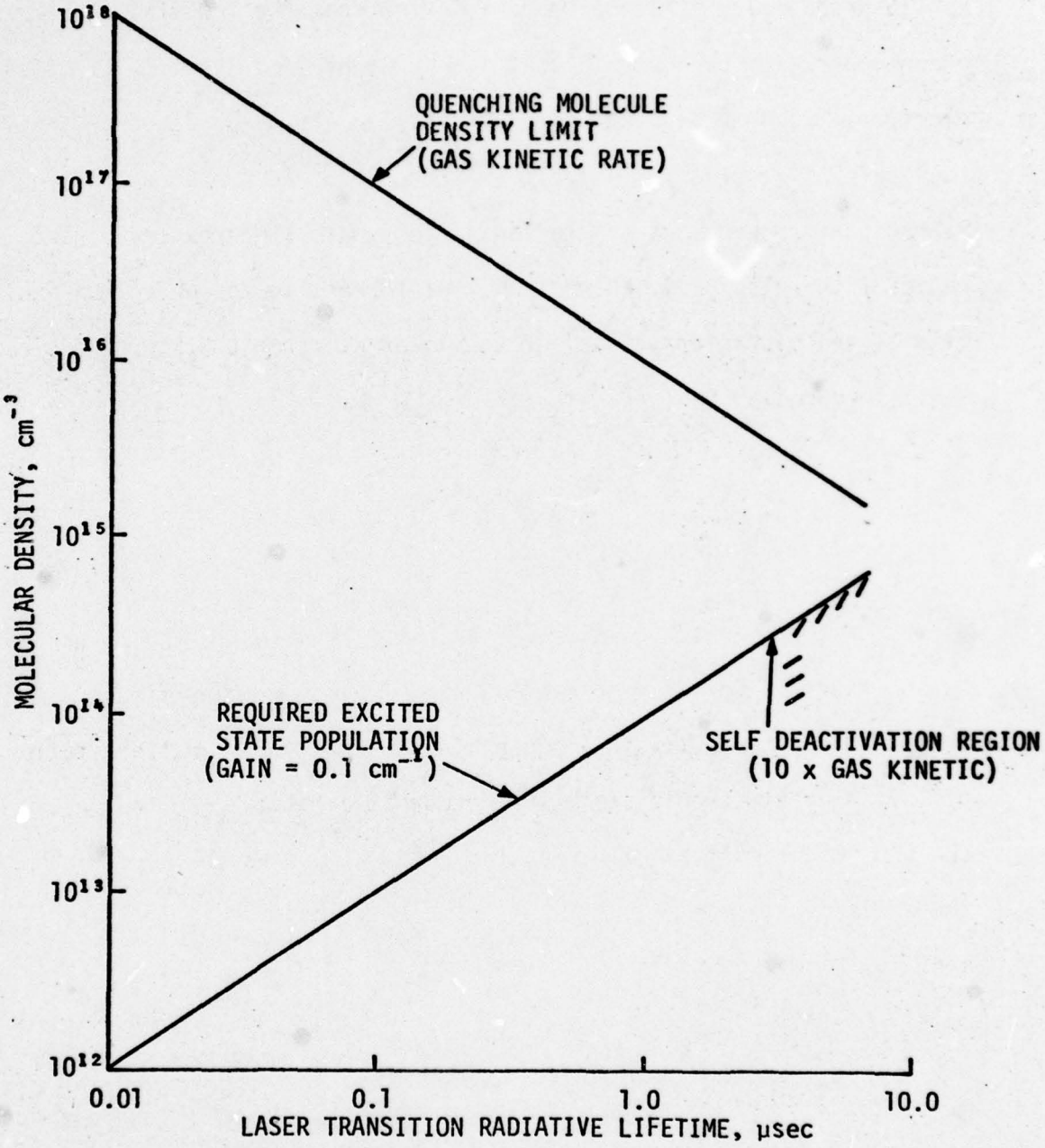

Figure 2. Competing Rate Processes for Collision Dominated Visible Electronic State Molecular Lasers

and a low vibrational temperature. In addition, a displacement of the minimum in the electronic potential curves is advantageous since it yields a high probability of spontaneous emission from the low vibrational levels of an upper electronic state to the upper vibrational levels of a lower electronic state (see Fig. 1). An inversion can be produced if the ratio of the electronic temperature of the two electronic states to the vibrational temperature of the lower electronic state exceeds the ratio of the electronic energy level difference to the energy of excitation of the vibrational level of the lower electronic state. This requirement is expressed by:

$$\frac{T_{el}}{T_v} > \frac{\Delta E_{el}}{\Delta E_v}$$

To achieve high specific laser power from the gas being used, it is necessary to recycle the excited laser molecules many times; this requires that the collisional quenching of the vibrational excitation of the lower electronic state must occur at a rate, k_{vib}, that exceeds the sum of the collisional quenching rate, k_{el}, plus the (spontaneous) radiative decay rate, A_{el}, of the upper electronic state. This requirement is expressed by:

$$\sum_i N_i \, k_{vib,i} > \sum_i N_i k_{el,i} + A_{el}$$

In order to achieve a collisional decay time of the lower laser level that is shorter than the radiative decay time of the upper laser level, the required minimum product of the collision probability times

the density of the quenching molecule is shown as the upper curve of Figure 2. Note that the actual required density is inversely proportional to the quenching probability.

The upper curve of Figure 2 also represents a maximum density-probability product for a gas component that causes collisional quenching of the upper electronic state. It should be noted, however, that the upper laser level may have a shorter total radiative lifetime than that due only to spontaneous emission corresponding to the laser transition. In this case the upper state quenching limit is increased by the ratio of the two radiative lifetimes.

It is seen from Figure 2 that the useful range of molecular electronic state radiative lifetimes lies between 0.01 and 10 μsec. It is also seen that the gas density requirements for collisional quenching are reasonable, provided favorable lower level vibrational quenching cross sections, ranging from 10^{-2} to 1 times gas kinetic, can be found.

A review of the presently available kinetic data on excited states of N_2 and CO was carried out in a search for favorable collisional quenching rates among the laser levels of these molecules. The results of this survey are summarized in Table I. It is seen that favorable possibilities exist for $N_2(B^3\Pi_g, v = 3)$ quenching by N_2 and for $CO(A^1\Pi, v = 1)$ quenching by He. It appears that the use of Ar with CO would yield poor results because of the high collisional quenching rate of the $B^1\Sigma^+$ state of CO by Ar. On the other hand, Ar is a good diluent for N_2, since it causes very little quenching of either the upper or the lower state. An additional candidate molecule for quenching the $N_2(B^3\Pi_g)$ state is C_2H_6 which has been observed

Table I

Summary of Collisional Quenching Data (cm^3/sec) for N_2 and CO Electronic States by Various Molecules

	Transition	λ(Å)	A_λ^{-1}(μsec)	K_Q(upper level)	k_Q(lower level)	References
N_2^*/He	$C^3\Pi_u \rightarrow B^3\Pi_g$	4058(0,3)	0.8	?	8×10^{-13}†	3
N_2^*/Ar	same	same	same	$< 3 \times 10^{-13}$	1.6×10^{-12}†	10, 3
N_2^*/N_2	same	same	same	1×10^{-11}	2.5×10^{-11}	4, 5
CO^*/He	$B^1\Sigma^+ \rightarrow A^1\Pi$	4835(0,1)	0.4	3.1×10^{-12}	1.5×10^{-11}	6, 7
CO^*/Ar	same	same	same	1.4×10^{-10}	1.6×10^{-10}	6, 7
CO^*/CO	same	same	same			

†unspecified v level.

to cause rapid vibrational quenching of the $N_2(A^3\Sigma_u^+)$ state (Ref. 2). This effect, together with the potential curve coincidence between the $A^3\Sigma_u^+$ state and the v = 3 level of the $B^3\Pi_g$ state of N_2 may lead to a rapid collisional quenching rate of the v = 3 level of the $B^3\Pi_g$ state. However, the collisional quenching rate of the $C^3\Pi_u$ state of N_2 by C_2H_6 is not yet known, and it may be quite large. The effect of adding C_2H_6 to N_2 in e-beam stabilized electric discharge experiments is discussed in Section 3.2.

SECTION III

TIME RESOLVED FLUORESCENCE STUDIES OF ELECTRONICALLY EXCITED STATES

3.1. Experimental Facility

The laser concepts described in the previous section have been studied using the 5-tube plasma diode electron-beam-stabilized electric discharge facility developed at MSNW in connection with VV transfer lasers (Ref. 1). A schematic diagram of this device is shown in Figure 3. The e-beam current density was approximately 50 mA/cm^2 and provided a stable discharge current density of 10 to 20 A/cm^2 at an E/N of 1 to 3 x 10^{-16} V-cm^2. The duration of the applied discharge could be varied from approximately 2 to 20 μsec and was normally applied at the peak of the e-beam current pulse. The N_2 or CO mole fractions varied from a few percent to as much as 25 percent for these gas mixtures. Total gas pressures ranged from as low as 20 torr to as high as 700 torr, although most of the work was done at approximately 200 torr.

Wavelength selection for the fluorescence studies was obtained by using a Jarrel-Ash 0.25 m Ebert Spectrometer equipped with gratings blazed at 600 nm and 2.1 μm. The ultraviolet and visible emission were detected with an RCA 1P28 photomultiplier tube (S-5 spectral response), while the near infrared emission was monitored with an RCA 7102 photomultiplier (S-1 spectral response). Both tubes were operated with a 50Ω signal cable terminated at the oscilloscope to provide fast time response.

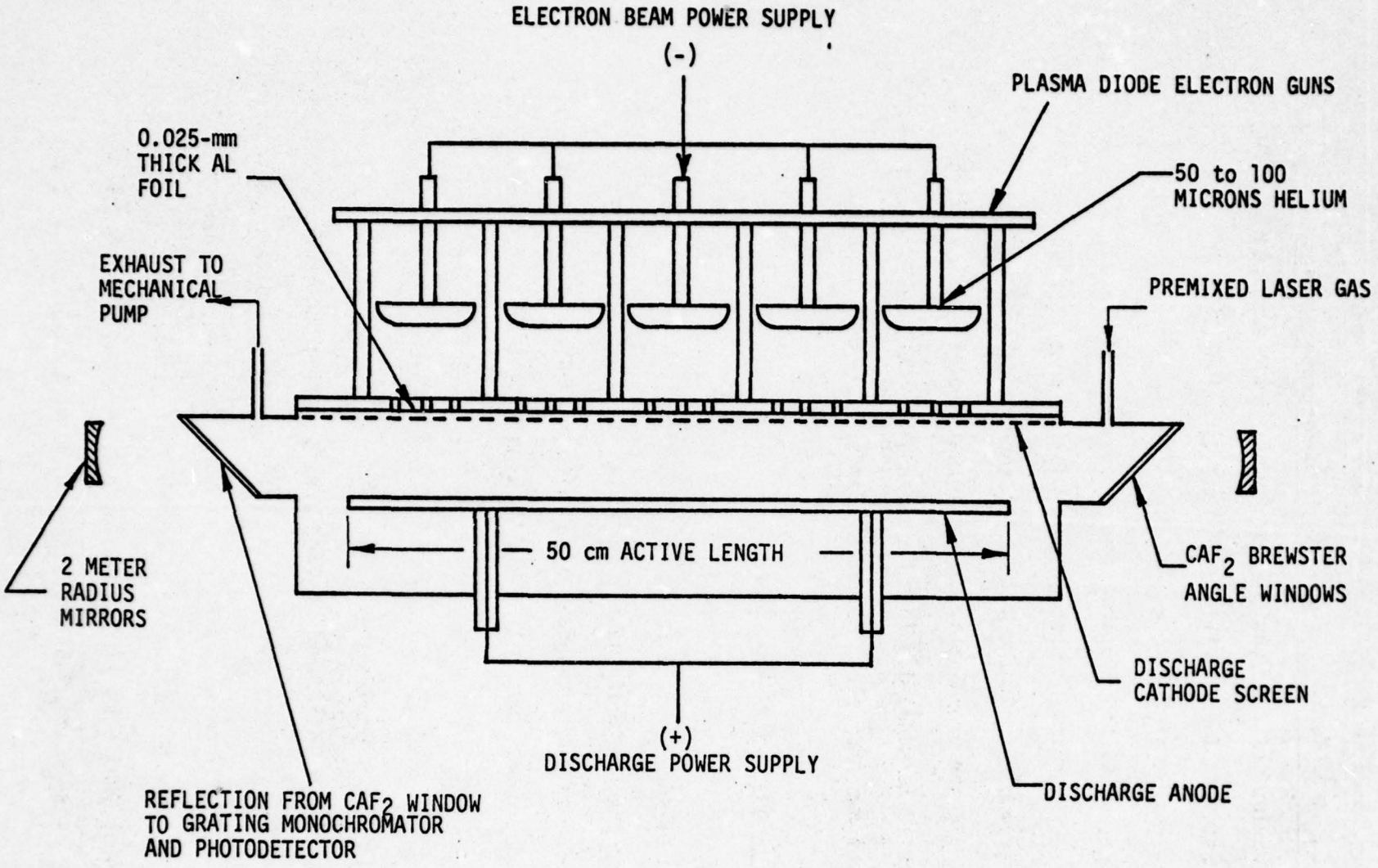

igure 3. Schematic of Five Tube Plasma Diode Electron-Beam-Stabilized Electric Discharge Cell and Laser Cavity. The anode-cathode spacing in the laser discharge cavity was 2.5 cm.

3.2. Summary of Results of Previous Fluorescence Studies

Previous studies (Ref. 1) of the fluorescence from the $B^3\Pi_g$ and $C^3\Pi_u$ states of N_2, utilizing a long duration (15 μsec) electric discharge pulse, showed both direct excitation processes (excitation transfer from Ar* and electron impact on ground state N_2) and a secondary indirect excitation process. The latter process resulted in a non-linear increase in the N_2 fluorescence emission during the discharge and a non-exponential decay of the fluorescence after the discharge is terminated. This has been interpreted as due to energy pooling of two $A^3\Sigma_u^+$ state molecules to form the $C^3\Pi_u$ state.

Effect of Addition of SF_6

In the earlier studies (Ref. 1) it was also found that the addition of small concentrations of SF_6 (~ 0.1%) to the gas mixture increases the ratio of the second positive emission to the first positive emission by an order of magnitude even though the discharge current decreases substantially. With no SF_6, the onset of arc formation limited the maximum obtainable E/N to a value of 1.3×10^{-16} V-cm^2 for an 85/15 Ar+N_2 gas mixture at 200 torr total pressure. However, the addition of approximately 0.1% SF_6 to the gas mixture resulted in an E/N of 2.1×10^{-16} V-cm^2 before arc formation occurred.

The effect of SF_6 addition on the discharge voltage, discharge current, and 3370 Å emission is shown in Figure 4. The discharge E/N in Figure 4(b) is approximately double that without SF_6 shown in Figure 4(a), while the discharge current is about an order of magnitude less in the SF_6 case. However, the ratio of the intensity of the 3370 Å

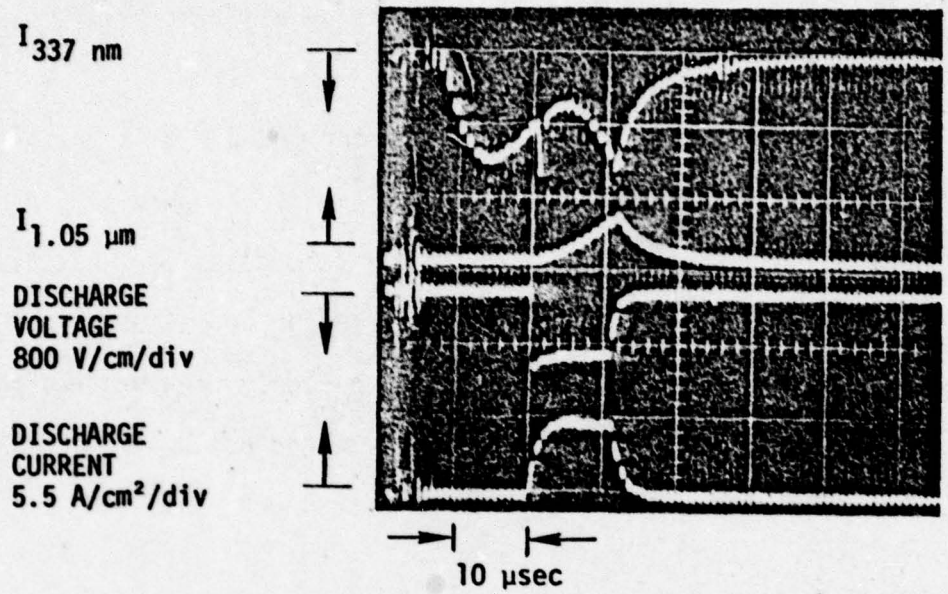

a) Ar + 15% N_2

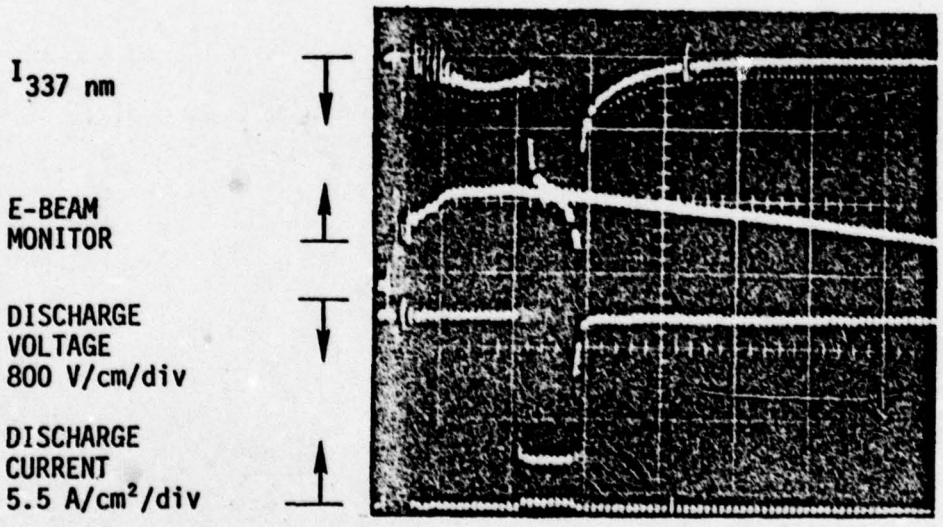

b) Ar + 15% N_2 + 0.1% SF_6

Figure 4. Effect of Small Concentrations of SF_6 on the Discharge Voltage, Discharge Current, and Fluorescence Emission for Ar/N_2 Mixtures at 200 torr

emission produced by the discharge to that produced by the e-beam has increased substantially.

The abrupt increase of the C → B emission when the discharge voltage is turned on is due to direct electron impact excitation of the C state. The emission then increases non-linearly during the discharge, most likely because of the increase in the A state density which populates the C state via the energy pooling reaction. When the discharge is terminated, the second positive emission drops abruptly due to the cessation of electron impact excitation. However, there is still a slowly decaying component to the C state emission after the discharge is turned off, which is probably produced by self collisions of the slowly decaying A state population.

Effect of Addition of C_2H_6

In previous attempts to obtain a long pulse $N_2(C \rightarrow B)$ laser, a collisional decay mechanism was suggested for the $N_2(B)$ state utilizing ethane (C_2H_6) (Ref. 1). This mechanism involves an intersystem potential curve crossing from the lower vibrational levels of the B state to the upper vibrational levels of the A state.

$$N_2(B^3\Pi_g) + N_2 \rightleftarrows N_2(A^3\Sigma_u^+)_{v=7} + N_2 + \Delta E$$

The rate constant for the formation of $N_2(A)v = 7$ reported by Dreyer and Perner (Ref. 2) is ~ 1×10^{-11} cm^3/sec. The $N_2(A)v = 7$ then decays somewhat more slowly down its own vibrational ladder until a bottleneck at the v = 3 and 4 levels is reached. The addition of small concentrations of C_2H_6 increases the rate of decay down the A state vibrational

ladder and removes the bottleneck at the v = 3 and 4 levels without having a significant effect on the A state population in lower vibrational levels (see Ref. 2).

These ideas were tested by observing the 3371 Å and 1 μm fluorescense with varying concentrations of C_2H_6 as a function of discharge E/N. However, the addition of C_2H_6 did not alter the ratio of second positive to first positive emission. The only observable effect due to the addition of C_2H_6 was the disappearance of the long time decay of both the 3371 Å and 1 μm emission. A typical trace is shown in Figure 5. The apparent implication of this observation is that C_2H_6 removes the A state; however, for the C_2H_6 concentrations used here, this would be inconsistent with the rate constant for electronic quenching of $N_2(A)$ reported by Dreyer and Perner (Ref. 2). One explanation for this inconsistency is that the long time decay component of the first and second positive emission may be formed primarily by energy pooling of A state molecules in higher vibrational levels, which are quenched rapidly by C_2H_6. This hypothesis could also help explain the disagreement in the reported values for the rate coefficient of the $N_2(A)$ state energy pooling reaction (see Ref. 8). A second explanation is the formation of other species from C_2H_6 in the discharge, which have a high $N_2(A)$ state quenching rate. This question can be resolved by making direct measurements of the populations of the individual vibrational levels of the $N_2(A)$ state.

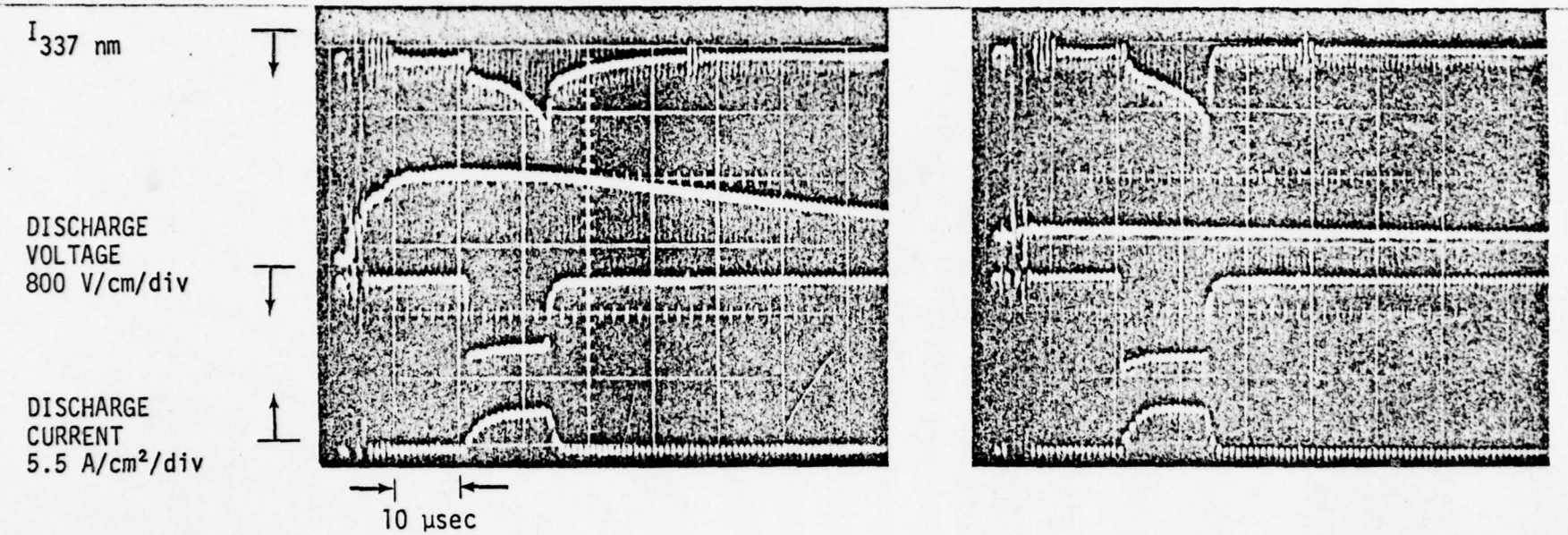

Figure 5. Effect of Ethane (C_2H_6) on the Emission from the (0,0) Band of the $N_2(C^3\Pi_u \rightarrow B^3\Pi_g)$ System for He+N_2 Mixtures at 200 Torr

3.3. Time Resolved Fluorescence from Specific Vibrational Levels of the $N_2(C^3\Pi_u)$ and $N_2(B^3\Pi_g)$ States

To gain further understanding of the kinetic processes occurring in high current discharges in Ar+N_2 and He+N_2 mixtures, we observed the time resolved fluorescence from individual vibrational levels of the nitrogen $C^3\Pi_u$ and $B^3\Pi_g$ states. The gas mixtures consisted of 15 to 20 percent N_2 in either He or Ar diluent at a total pressure of 200 torr. The fluorescence was produced in the e-beam stabilized electric discharge facility described in Section 3.1. The discharge voltage was applied near the peak of the e-beam current pulse and was terminated after 5 to 10 μsec. The electric discharge energy storage circuit was modified to reduce the inductance and provide a short (2 μsec) rise time of the current. The values of E/N were 1.2 x 10^{-16}V-cm^2 and 1.7 x 10^{-16}V-cm^2 while the discharge currents were 18 A/cm^2 and 6.6 A/cm^2 for the Ar+N_2 and He+N_2 mixtures, respectively. The applied voltage was slightly below the value that would cause an arc near the end of the discharge pulse.

Nitrogen $C^3\Pi_u \rightarrow B^3\Pi_g$ Fluorescence

Fluorescence emission from the v= 0 level of the $N_2(C^3\Pi_u)$ state is shown in Figure 6. The upper trace shows the emission produced by the e-beam, while the lower trace shows the effects of the discharge on this emission. The C state emission due to the e-beam is probably produced by energy transfer from excited argon atoms which result from dissociative recombination of Ar_2^+ ions. From Figure 6 it is apparent that the v = 0 fluorescence of the nitrogen C state decreases abruptly when the discharge voltage is applied. As the discharge current increases,

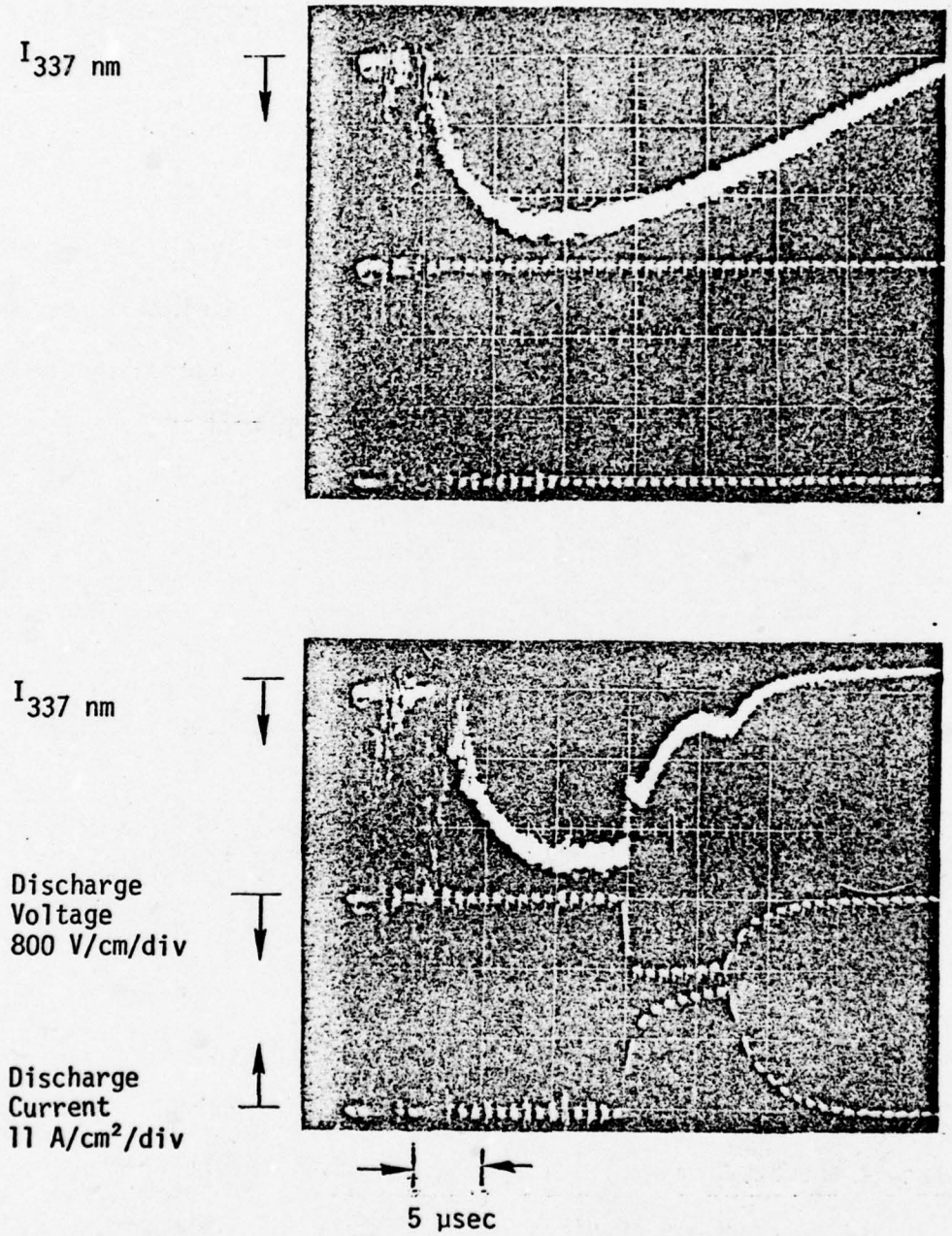

Figure 6. Fluorescence Emission from the v = 0 Level of the $N_2(C^3\Pi_u)$ State. The upper oscillogram shows the emission produced by the e-beam; the lower oscillogram shows the effect of the discharge on this emission.

the C state emission increases slightly and then falls during the next 3 or 4 μsec. The emission then increases non-linearly until the discharge is terminated, after which the fluorescence decays with a time constant much longer than the C state radiative lifetime.

The abrupt drop in the C state emission is most likely due to a decrease in the Ar^* population density caused by a decrease in the dissociative recombination rate when the electron temperature is increased by the application of the discharge voltage. The more gradual decrease in the C state emission during the early part of the discharge may be due to the production of some species which is an efficient deactivator of excited argon atoms or it may be due to a further reduction in the rate of producing excited argon atoms. This premise is supported by the observation that the C state emission due to the e-beam remains quenched even after the discharge has been terminated and the electrons have had a chance to cool. Further work would be necessary in order to identify the species and the process responsible for this interference in the nitrogen C state production channels.

In wavelength scanning experiments we have observed that the relative intensities of the emission from the v = 0 level of the nitrogen $C^3\Pi_u$ state produced by the e-beam and by the electric discharge vary with wavelength within an emission band. The emission produced by the e-beam is peaked at longer wavelengths, while that produced by the electric discharge is peaked at shorter wavelengths. This suggests that two distinct processes are responsible for this emission and that they result in different rotational distributions for the C state. Since

individual rotational lines were not resolved, no quantitative information about these distributions was obtained.

In Figure 7, fluorescence emission from the v = 0 and v = 1 levels of the nitrogen $C^3\Pi_u$ state is compared. The difference is striking. Although the v = 1 emission produced by the e-beam drops abruptly when the discharge voltage is applied, it quickly recovers as the discharge current rises and then increases non-linearly until the discharge is terminated. The electric discharge is evidently more effective than the high energy electron beam at producing the v = 1 level of the C state, although the e-beam produces the v = 0 level more strongly than the electric discharge does.

In the preceding section it was indicated that the non-linear increase and long time decay of the C state fluorescence were attributable to the energy pooling reaction

$$N_2(A^3\Sigma_u^+) + N_2(A^3\Sigma_u^+) \rightarrow N_2(C^3\Pi_u) + N_2(X^1\Sigma_g^+)$$

Since $N_2(A^3\Sigma_u^+)$ self collisions produce the v = 1 and v = 0 levels of the $N_2(C)$ state with roughly equal probability (Ref. 9), excitation transfer from Ar^* must favor the v = 0 level of the C state. These observations are consistent with the results of Setser, Stedman, and Coxon (Ref. 10), who report that excitation transfer from $Ar(^3P_{0,2})$ to N_2 favors the production of $N_2(C^3\Pi_g)$ v = 0 with a non-equilibrium rotational distribution.

When $He+N_2$ mixtures are excited, the behavior of the v = 0 and v = 1 levels is similar. Fluorescence arising from the same transitions shown in Figure 7 for $Ar+N_2$ mixtures is shown in Figure 8 for 5:1 $He+N_2$

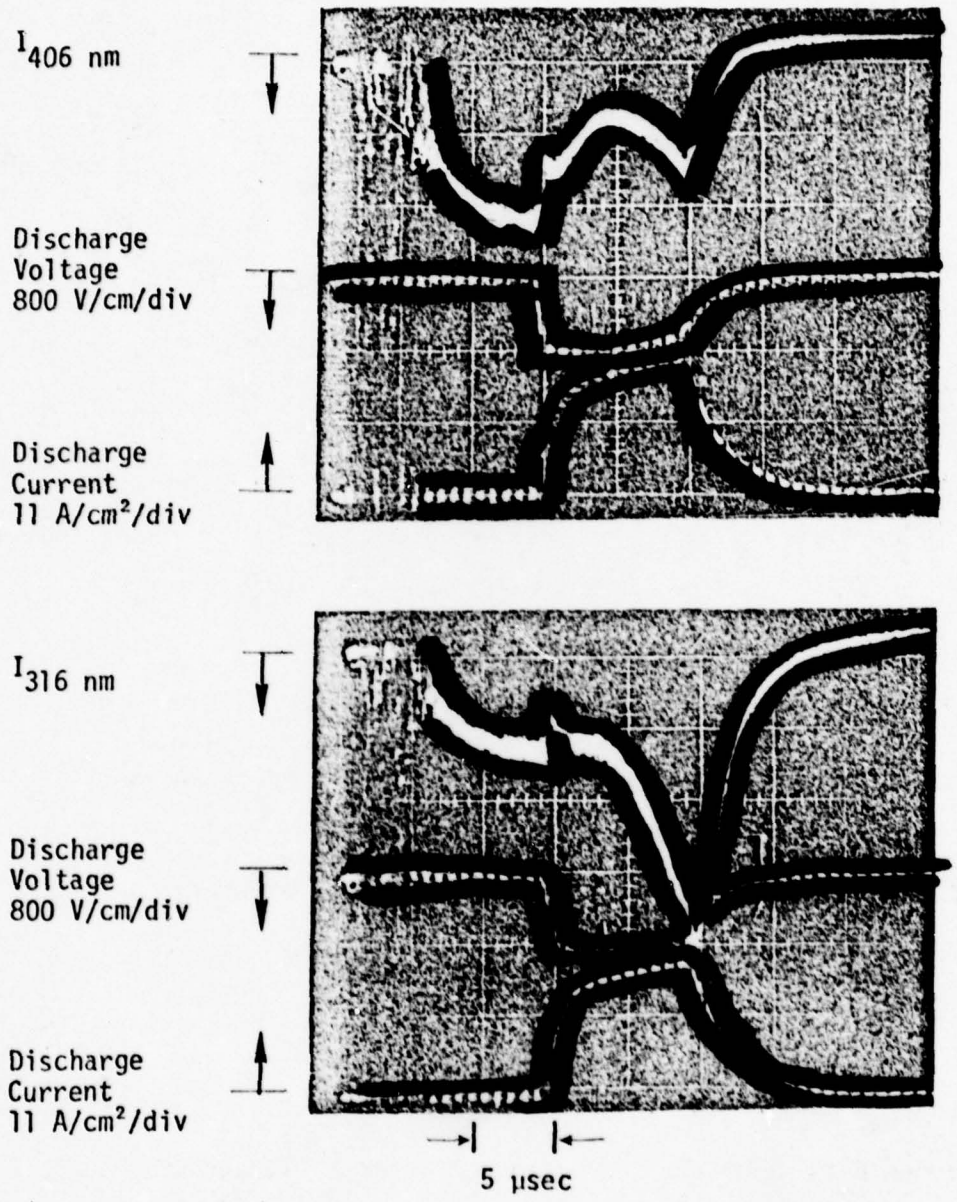

Figure 7. Comparison of Fluorescence Emission from the v = 0 and v = 1 Levels of the $N_2(C^3\Pi_u)$ State in a 5:1 Ar+N_2 Mixture at 200 Torr. The upper oscillogram shows the (0,3) band and the lower oscillogram shows the (1,0) band of the nitrogen second positive system.

mixtures. It is apparent that there is very little C state emission produced by the e-beam. During the discharge, the C state fluorescence increases non-linearly until the discharge is terminated, after which the emission decays with a time constant much longer than the C state radiative lifetime. As in the case of $Ar+N_2$ mixtures, the electric discharge produces substantial excitation of the v = 1 level of the C state.

In Figure 8, an abrupt drop in C state emission is seen at the time of termination of the discharge voltage. However, there was no abrupt rise in C state emission at the onset of the discharge voltage. This suggests that direct electron impact excitation of the C state increases during the pulse. This may be due to a shift in the electron distribution function to higher energies, as vibration of N_2 becomes excited, or it may be due to the buildup of the A state population, permitting electron impact with the A state to produce the C state. Both of these explanations illustrate how the energy deposition in the gas may have an important effect on the rate of excitation (and ionization) of the gas at low or moderate values of E/N. The volume rate of ionization in turn plays a major role in arc breakdown of these discharges.

Nitrogen $B^3\Pi_g \rightarrow A^3\Sigma_u^+$ Fluorescence

We have observed fluorescence from the v = 0, 1, and 2 levels of the nitrogen B state and find that it is essentially the same in both $He+N_2$ and $Ar+N_2$ mixtures. There is very little emission produced by the e-beam for any of these levels. During the discharge, the fluorescence from the v = 0, 1, and 2 levels increases linearly until the discharge is terminated, after which it decays. Oscilloscope traces showing the

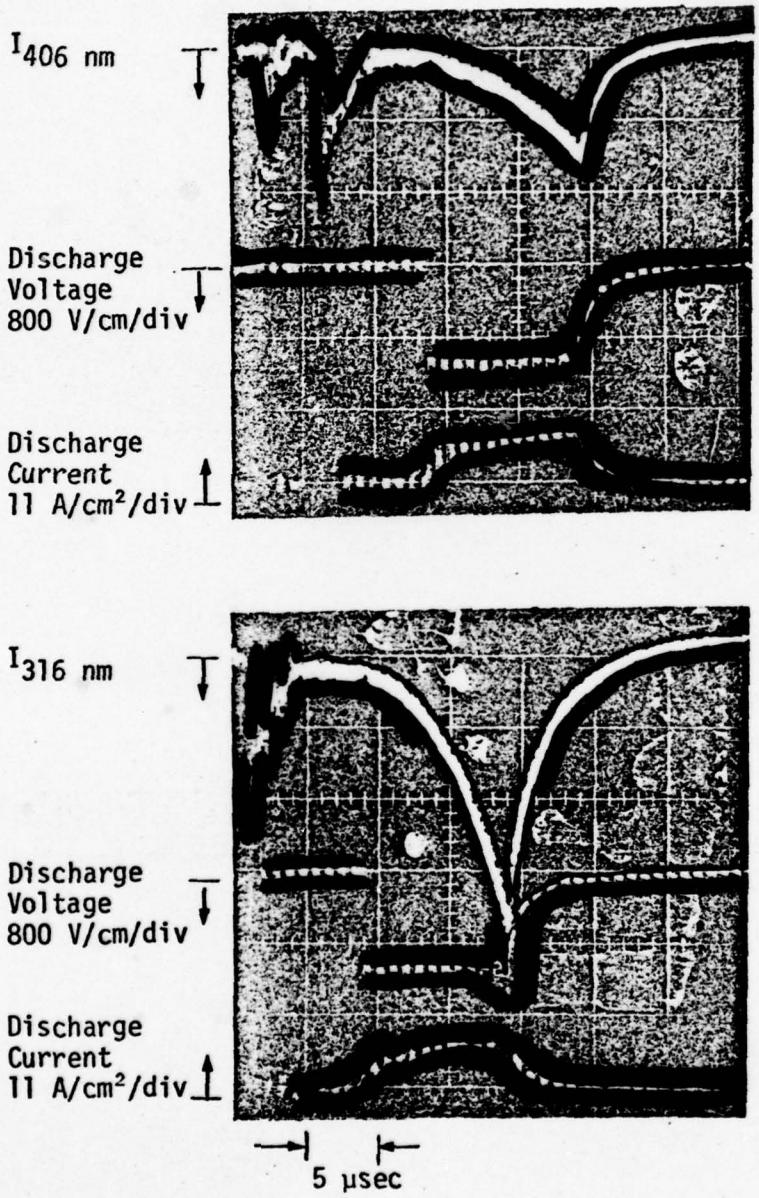

Figure 8. Comparison of Fluorescence Emission from the v = 0 and v = 1 Levels of the $N_2(C^3\Pi_u)$ State in a 5:1 He+N_2 Mixture at 200 Torr. The upper oscillogram shows the (0,3) band and the lower oscillogram shows the (1,0) band of the nitrogen second positive system.

time history of the fluorescence from the v = 0 and v = 1 levels of the $N_2(B^3\Pi_g)$ state are shown in Figure 9 for 5:1 Ar+N_2 mixtures. The B state emission shows no resemblance to the emission from the C state (Fig. 7), nor to the integral of the C state emission, indicating that radiative cascade from C to B is not the only production mechanism for the B state. Evidently, the most important production process for the B state is direct excitation by electron impact with the ground state of N_2.

Several important observations have resulted from this work which bear on the production of a long pulse laser based on the second positive system of N_2. From our observations of the fluorescence from various vibrational levels of the N_2 (C and B) states, it is evident that electric discharge excitation from below produces significant vibrational excitation of the excited electronic states for the conditions of the present investigation. Significant vibrational excitation is undesirable both from the standpoint of efficiency and because we are trying to achieve an inversion based on a high electronic temperature and a low vibrational temperature. Thus it appears that excitation from above (e.g., recombination of ions produced by a high energy electron beam) may be a more effective means of producing a large population in relatively high lying electronic states without obtaining significant vibrational excitation. However, it should be pointed out that the vibrational fluorescence measurements were carried out with gas mixtures having a large fraction of N_2 (approximately 16 to 20 percent). The applied electric field was limited to a low value by arc breakdown for the pulse duration used, and led to a low electron temperature. By reducing the N_2 fraction, decreasing the pulse

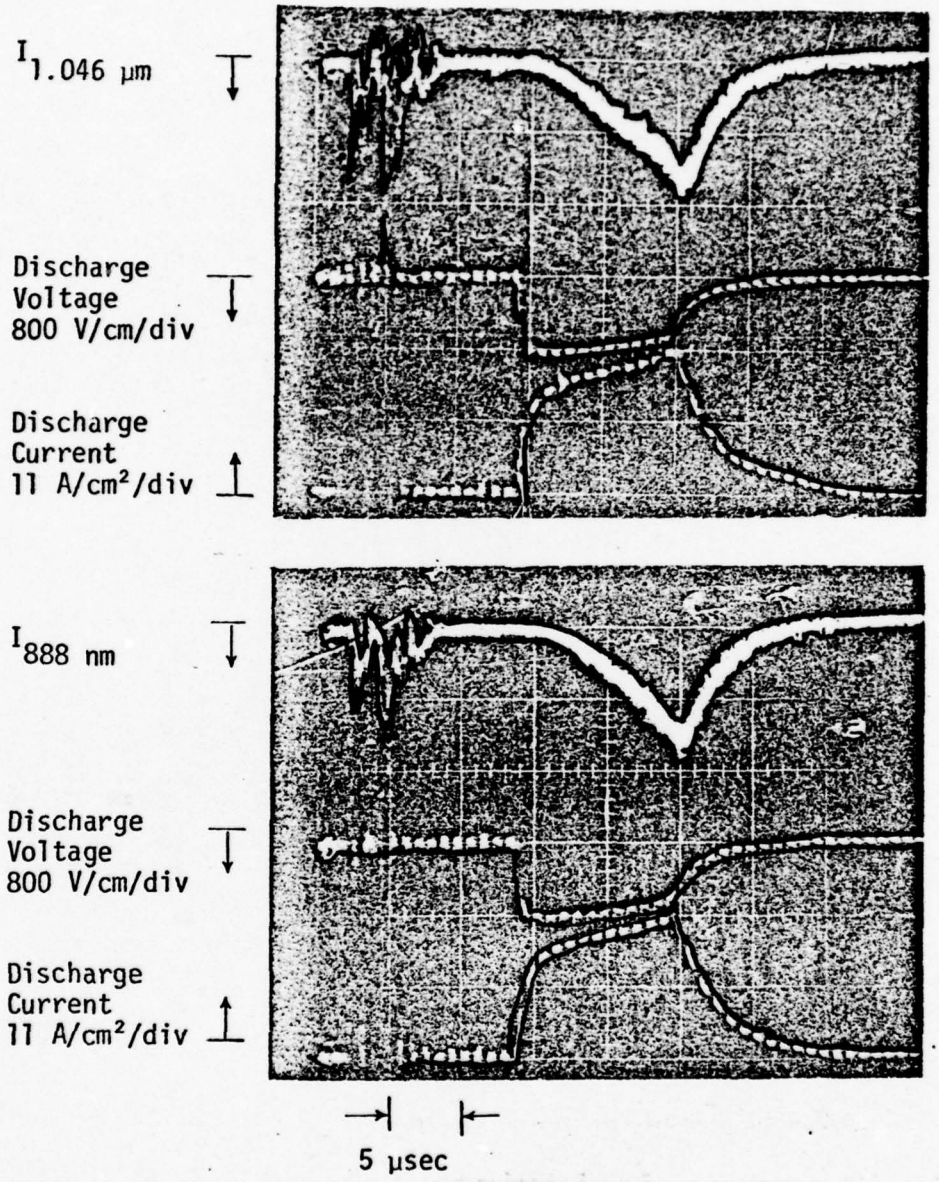

Figure 9. Fluorescence Emission from the v = 0 and v = 1 Levels of the $N_2(B^3\Pi_g)$ State in a 5:1 Ar+N_2 Mixture at 200 Torr. The upper oscillogram shows the (0,0) band and the lower oscillogram shows the (1,0) band of the nitrogen first positive system.

duration, and raising the applied voltage, it should be possible to put a much larger fraction of the electric discharge energy into electronic excitation.

In light of the large production rate of the $N_2(C^3\Pi_u)$ v = 1 level observed in the case of electric discharge excitation, the (1,3) band of the nitrogen second positive system becomes an attractive candidate for a long pulse visible laser. In a 97:3 Ar+N_2 mixture at atmospheric pressure, the v = 3 level of the $N_2(B^3\Pi_g)$ state would be collisionally deactivated much more rapidly than the (1,3) and (0,3) radiative lifetimes for the C → B transition. In addition, the transition probability for the (1,3) band of the second positive system is approximately 0.4 of the transition probability for the (0,0) band and thus the population inversion density for the (1,3) band only needs to be a factor of 2.5 greater than for the (0,0) band in order to have the same gain.

SECTION IV

ABSOLUTE POPULATION MEASUREMENTS

In order to assess quantitatively the excitation efficiency of specific electronic states, or to evaluate the kinetic mechanisms taking place in electrically excited gas laser mixtures, it is necessary to determine the absolute population densities of the excited states of interest as a function of time during and after the discharge. It was decided to use probe laser absorption whenever possible, and to supplement this technique with absolute emission spectroscopy on those states for which a convenient probe laser is not available. For the nitrogen system, the population densities of the lower vibrational levels of the metastable $N_2(A^3\Sigma_u^+)$ state were probed by a laser operating on the N_2 first positive system ($B^3\Pi_g \rightarrow A^3\Sigma_u^+$). In addition, a general technique for the determination of the population densities of electronically excited states using a narrow bandwidth, tunable, dye laser has been designed and is under development. This technique and the results obtained for the $N_2(A)$ state are described in the following sections.

4.1. $N_2(A^3\Sigma_u^+)$ Population Density Measurement

Population densities for the v = 0 and v = 1 levels of the metastable $N_2(A^3\Sigma_u^+)$ state have been determined as a function of time during and after an e-beam stabilized electric discharge pulse. This was accomplished by measuring the absorption of a beam from a probe laser

operating on the (1,0) and (2,1) bands of the nitrogen $B^3\Pi_g \rightarrow A^3\Sigma_u^+$ transition at 888.8 nm and 870.0 nm, respectively. The probe laser consisted of a resistor loaded pin discharge having an active length of 1.4 m. The electrical energy was obtained from a charged capacitor switched by a triggered spark gap. This combination resulted in a discharge current rise time of about 0.1 μsec and a pulse duration of approximately 0.5 μsec. The gas mixture for the probe laser consisted of 10 torr nitrogen and 40 torr helium and was continuously flowed through the laser tube. The semi-confocal optical cavity was formed by a flat reflector and a 3 m radius of curvature, hole coupled mirror, both of which were gold coated.

The optical arrangement for the absorption measurements is shown schematically in Figure 10. Two optical detectors were employed, one to monitor the laser output on each pulse and the other to record the signal transmitted through the e-beam stabilized electric discharge chamber. The reference detector was an RCA 7102 photomultiplier tube (S-1 spectral response) and the signal detector was an RCA C31034 photomultiplier tube with a spectral response extending out to 930 nm. The anode signals from both tubes were transmitted to the oscilloscope via 50 Ω coaxial cable terminated at the receiving end. The reference signal was obtained by splitting off a portion of the incident probe laser emission with a partially reflecting mirror and then using a grating for selecting the same wavelength that the monochromator was viewing. Nylon scatterers were placed in front of the monochromator slit and the iris diaphram in front of the reference detector in order

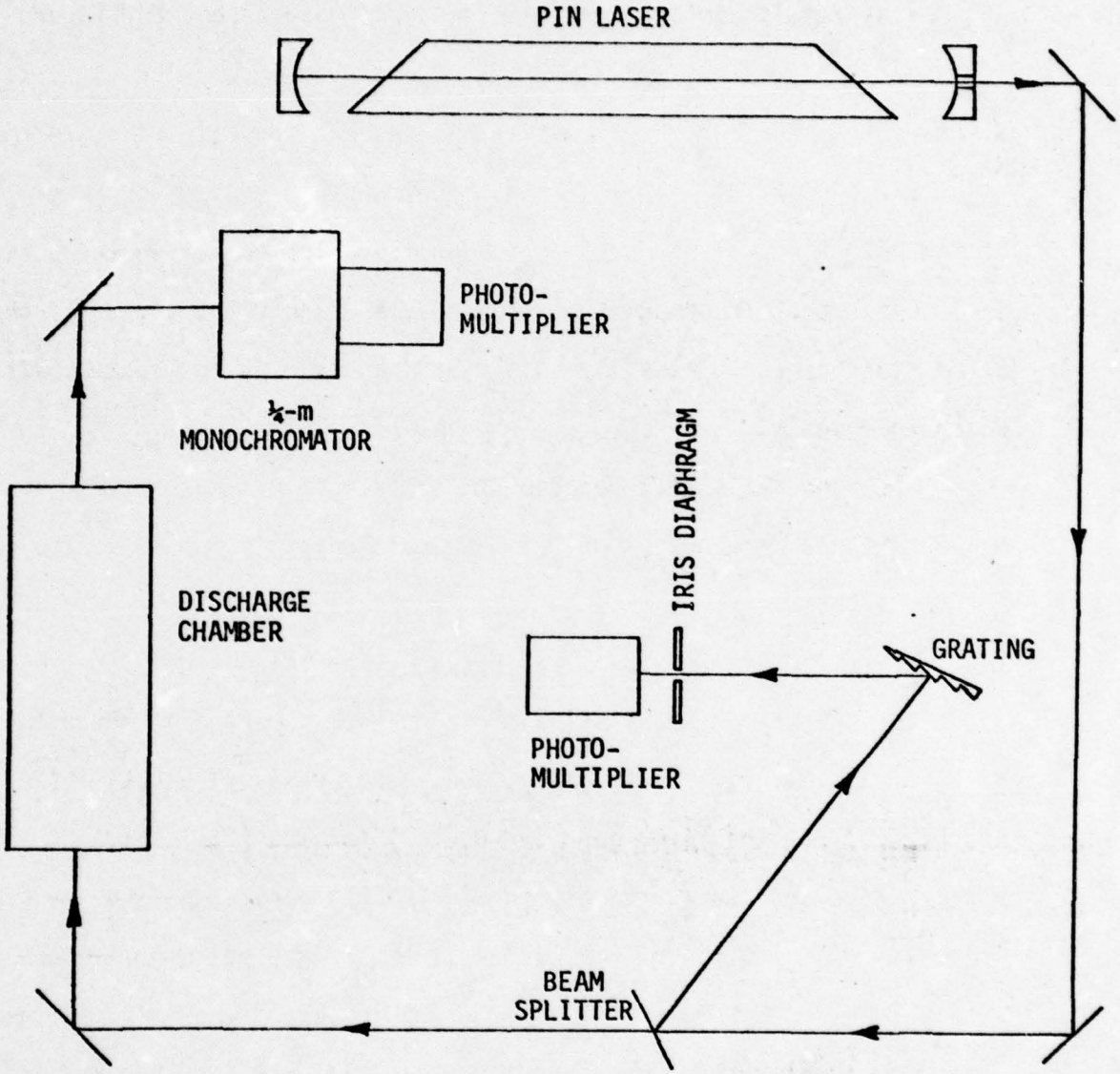

Figure 10. Optical Arrangement for Probe Laser Absorption Determination of $N_2(A^3\Sigma_u^+)$ Population

to minimize effects due to deflection of the probe laser beam that might be caused by gas motion during long excitation pulses.

The results obtained with this technique are shown in Figure 11 for an Ar + 17% N_2 mixture at 200 torr total pressure. The electric discharge was applied for 8 μsec with a power input rate of 13 kW/cm^3 at an E/N of 1.2 x 10^{-16}V-cm^2. This represents an energy input of 0.1 eV/molecule. Although there is considerable scatter in the data, it is clear that the populations of the v = 0 and v = 1 levels of the $N_2(A)$ state increase steadily until the discharge is terminated, after which they decay.

Interpretation of the absorption measurements has been carried out on the assumption that only a single rotational line is emitted by the probe laser. While this is certainly not correct, this simplification seems to be justified on the basis of the following discussion. The most intense rotational line for each band reported in the detailed study of the molecular nitrogen pulsed laser by Kasuye and Lide (Ref. 11) was Q_{11} (9) for the (1,0) band and Q_{11} (7) for the (2,1) band. Furthermore, Kasuye and Lide were able to fit their experimentally observed intensity distribution of rotational lines for the pulsed nitrogen laser with a rotational temperature of 325 °K (Ref. 11). The lack of significant rotational heating suggests that this will not be a problem in the probe laser. The results suggest that the probe laser may be characterized by a room temperature distribution of rotational states, and, if the absorbing gas is also characterized by a room temperature rotational distribution, the principal absorption will be on the same levels that are emitted most strongly by the probe laser. For this reason, the

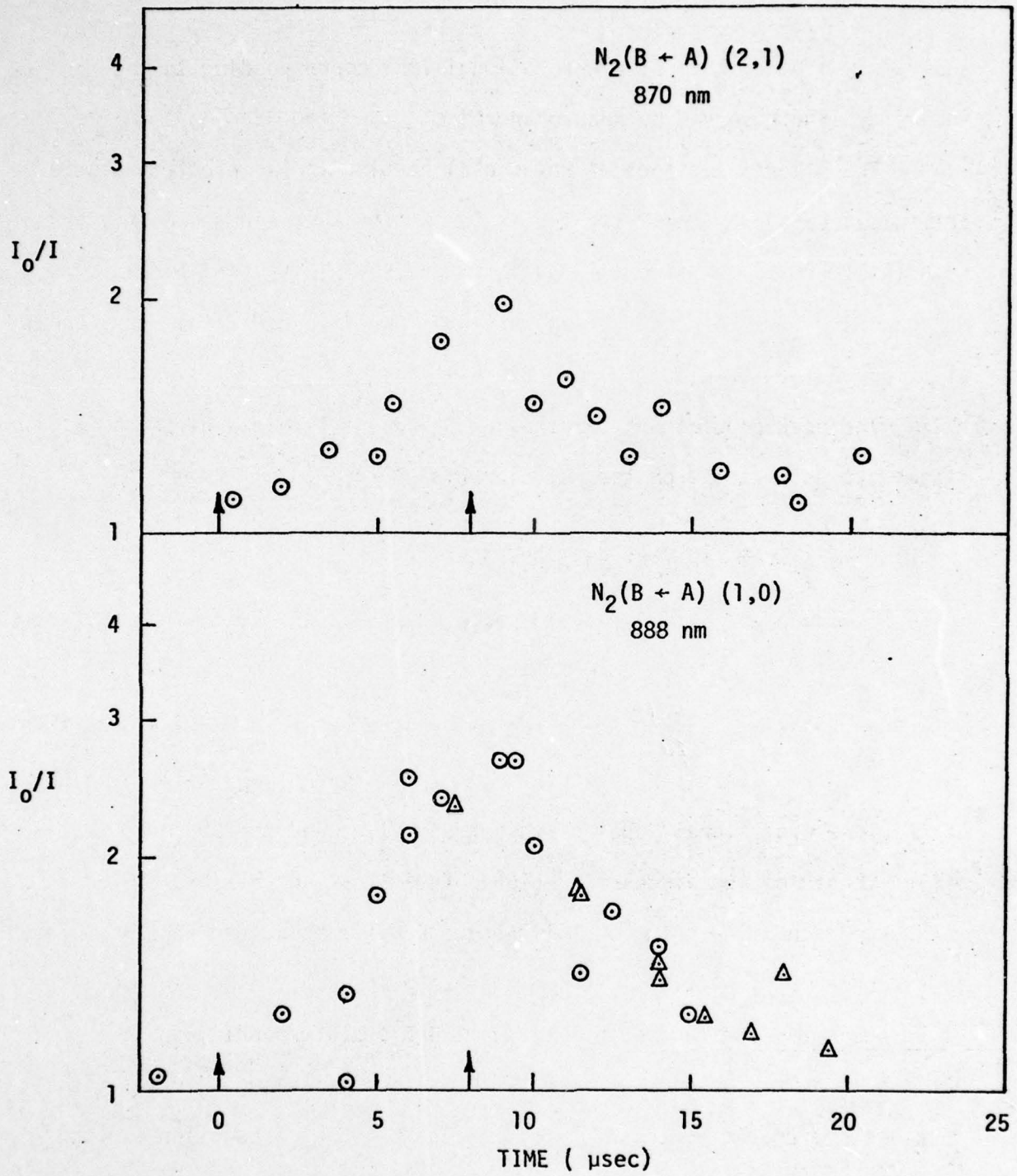

Figure 11. Probe Laser Absorption Measurements for the (2,1) and (1,0) Bands of the Nitrogen First Positive System at Different Times During and After the Electric Discharge

analysis was based on a single rotational line corresponding to the maximum intensity line observed by Kasuye and Lide.

The potential effect of rotational heating in the electric discharge cell was assessed by repeating the analysis with the assumption that the rotational and translational temperature of the $N_2(A)$ state in the absorption cell was 400 °K. This assumption increases the inferred total vibrational state population by about 20 percent.

The peak populations for the v = 0 and v = 1 levels of the $N_2(A)$ state were estimated from the relationship

$$I_{tr} = I_o \exp(-\alpha_{J"J'} N_{v"K"J"} \ell)$$

where I_o is the incident intensity of the probe laser beam, I_{tr} is the intensity of the probe laser beam transmitted through the electric discharge cell, $\alpha_{J"J'}$ is the absorption cross section for an individual rotational transition v'K'J' ← v"K"J", $N_{v"K"J"}$ is the population density of the lower rotational level of this transition, and ℓ = 50 cm is the active length of the discharge region. In evaluating this expression it was assumed that the rotational lines are Doppler broadened and that there is no overlapping of lines within the absorption cell. The contribution of stimulated emission due to a large $N_2(B^3\Pi_g)$ state population was neglected; an underestimate of the $N_2(A^3\Sigma_u^+)$ population would result if this assumption were not correct. The absorption cross section for the peak of the Doppler profile was then calculated using the following expression

$$\alpha_{J''J'} = \frac{1}{\Delta\nu_D}\left(\frac{\ln 2}{\pi}\right)^{\frac{1}{2}} \frac{\lambda^2_{J'J''}}{4\pi} A_{v'v''} \frac{S_J}{2J''+1} \left(\frac{\lambda_{v'v''}}{\lambda_{J'J''}}\right)^3$$

where $\Delta\nu_D$ = Doppler width of rotational transition

$\lambda_{J'J''}$ = wavelength of the rotational transition

$\lambda_{v'v''}$ = wavelength of the v' → v" band origin

$A_{v'v''}$ = transition probability for the v' → v" band of the electronic transition

S_J = rotational line strength of the J' ← J" transition

Values of the transition probability for the (1,0) and (2,1) bands of the nitrogen first positive system were taken from Shemansky and Broadfoot (Ref. 12) and are $A_{10} = 8.72 \times 10^4$ sec^{-1} and $A_{21} = 6.17 \times 10^4$ sec^{-1}. The rotational line strength S_J was calculated from the formula tabulated by Schadee (Ref. 13), using the coupling constant Y = 25.8 reported by Budò (Ref. 14). The population of the individual rotational state $N_{v''K''J''}$ can be related to the total population of the vibrational level $N_{v''}$ according to

$$N_{v''K''J''} = 2\phi\,(2J+1)\exp(-hcF(K)/kT)\,N_{v''}/(2S+1)\,Q_{rot}$$

where S is the electronic spin angular momentum, Q_{rot} is the rotational partition function, $F(K) = B_v K(K+1)$, and ϕ is the nuclear spin statistical weight factor, which for N_2 has the value 2/3 for symmetric rotational levels and 1/3 for antisymmetric rotational levels. Relating the two populations in this manner assumes that the $N_2(A)$ state molecules in the discharge cell are in rotational equilibrium at the temperature T.

The peak population of the v = 0 and v = 1 levels of the $N_2(A^3\Sigma_u^+)$ state estimated as outlined above are both approximately 10^{14} molecules/cm^3. This suggests that electric discharge excitation

produces substantial vibrational excitation of the excited electronic state, in agreement with the results of the fluorescence studies on the $C^3\Pi_u$ and $B^3\Pi_g$ states.

The decay of the $N_2(A)$ state after the discharge has been terminated can be represented by the equation

$$-\frac{dA}{dt} = k_p A^2 + \lambda_q A \quad \text{where } \lambda_q = \tau_A^{-1} + \sum_i k_{qi} Q_i$$

Here k_p is the rate coefficient for $N_2(A)$ deactivation due to self collisions, τ_A is the A state radiative lifetime, and k_{qi} and Q_i are, respectively, the A state quenching rate coefficient and the concentration of the i^{th} component of the mixture. If it is assumed that the A state decay is due to the energy pooling reaction, then the above equation has the approximate solution

$$A \sim (A_o^{-1} + k_p t)^{-1}$$

where A_o is the $N_2(A)$ population at $t = 0$. Thus a plot of A^{-1} as a function of t should give a straight line whose slope is k_p. The value of k_p determined from the data of Figure 11 is about 3×10^{-9} cm^3/molecule-sec, which is in approximate agreement with the value of 1.4×10^{-9} cm^3/molecule-sec reported by Hays and Oskam (Ref. 15).

From the measured population densities it is possible to estimate the excitation efficiency of the $N_2(A)$ state due to the electric discharge. By putting together measurements for different gas mixtures and pulse durations, it was possible to plot the $N_2(A)$ state excitation efficiency as a function of E/N. These data are presented in Figure 12.

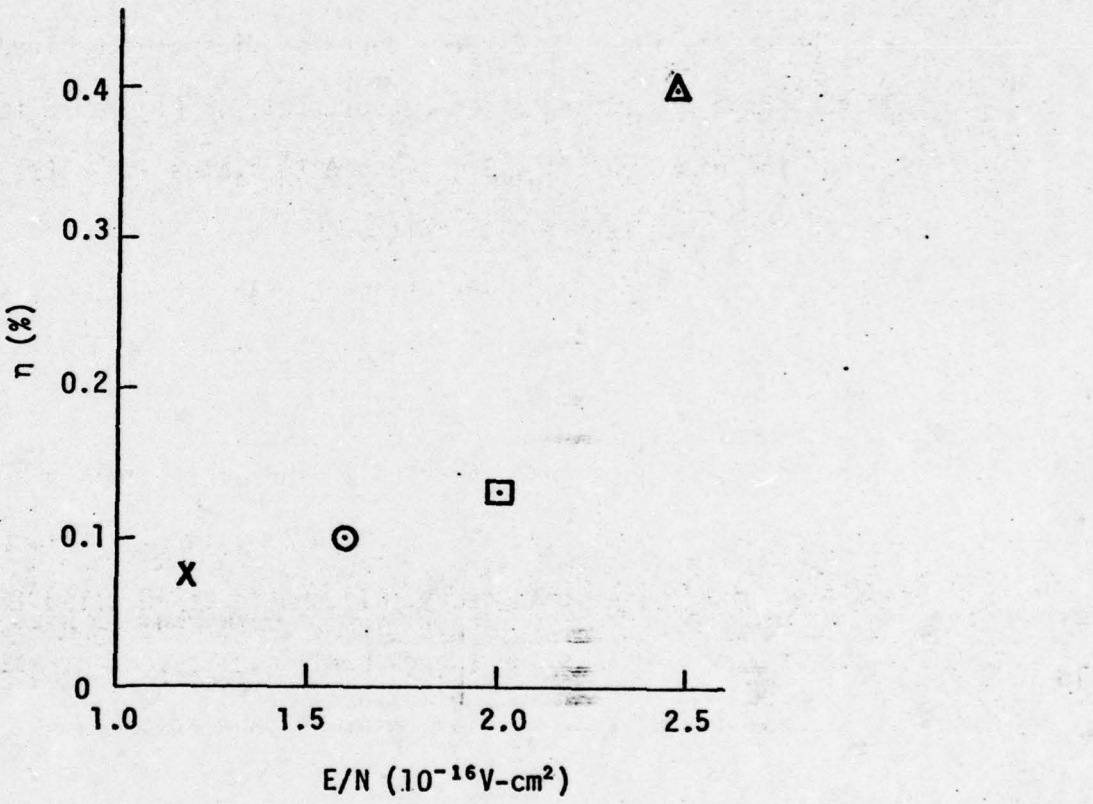

Figure 12. Excitation Efficiency of $N_2(A^3\Sigma_u^+)$ as a Function of E/N for Various Gas Mixtures and Discharge Conditions

Although no absorption measurements were made for the Ar + 15% N_2 + 0.1% SF_6 mixture, the $N_2(A)$ state population was estimated by comparing the $N_2(C)$ state decay with that obtained for the experiments in which the A state population was measured. The efficiencies are disappointingly small, but the dependence on E/N suggests that they can be improved significantly by increasing the applied voltage. The principal experimental difficulty in doing this is the onset of the glow to arc transition.

Data from the fluorescence decay studies are combined with those from the probe laser absorption measurements in Figure 13 to show the decay of the nitrogen $C^3\Pi_u$, $B^3\Pi_g$, and $A^3\Sigma_u^+$ states after the electric discharge has been terminated. Although the earlier C and B state fluorescence decay studies were obtained with a much lower energy input rate, the similarity of the A, B, and C state decay is evident. Also shown in the figure are data for the C state decay taken under the same conditions as the A state absorption measurements. The square root of this decay curve is plotted as the solid line in Figure 13 (c) for comparison with the A state decay. It should be recalled that if the C state is formed by A state energy pooling, its concentration will be proportional to the square of the A state population.

4.2. Tunable Dye Laser Diagnostic Technique

The tunable dye laser is a very convenient and general light source for determining populations of excited electronic states that are non-radiating or that are otherwise difficult to measure. In addition to tunability the coherence, high spectral brightness, directionality, and narrow bandwidth of the dye laser offer significant advantages over conventional light sources for absorption spectroscopy.

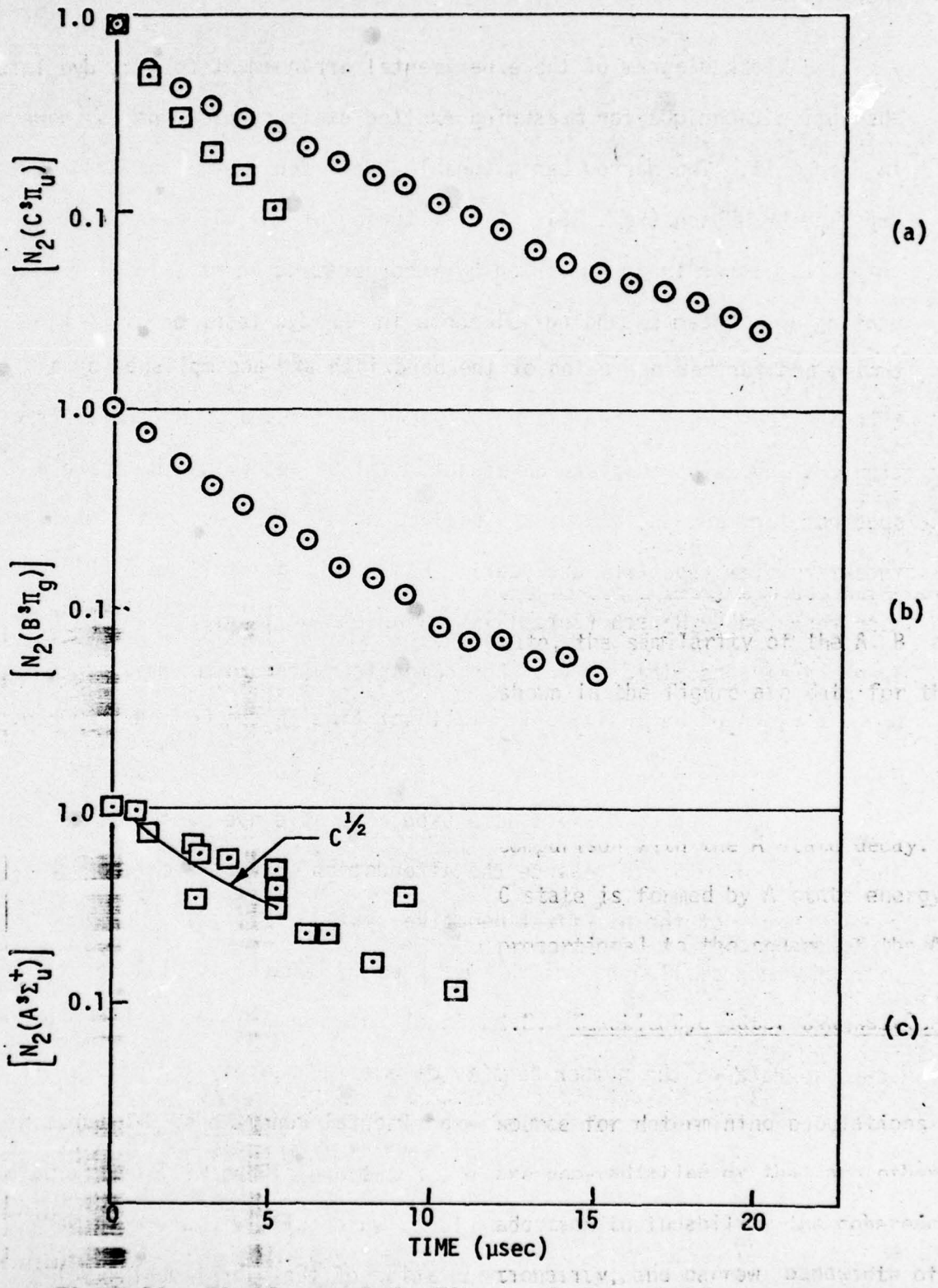

Figure 13. Time Decay of the Nitrogen A, B, and C States After the Electric Discharge Has Been Terminated

⊙ Ar + 15% N_2 at 200 Torr, P_{in} = 4.4 kW/cm³

⊡ Ar + 17% N_2 at 200 Torr, P_{in} = 13 kW/cm³

A block diagram of the experimental arrangement for the dye laser absorption technique for measuring excited state populations is shown in Figure 14. The narrow band, tunable dye laser is the same as that reported by Hänsch (Ref. 16). Coarse tuning of the nitrogen laser pumped dye laser is accomplished by incorporating an echelle diffraction grating and a beam expanding telescope in the dye laser cavity. Fine tuning and further narrowing of the bandwidth are accomplished by a tilted Fabry-Perot etalon placed between the telescope and the diffraction grating. The absolute wavelength will be determined by using a spectrometer, and the bandwidths will be obtained by using a high finesse interferometer (spectrum analyzer). Bandwidths as small as 0.004 Å have been reported by Hänsch (Ref. 16) when an etalon is placed in the dye laser cavity described above. For comparison, the room temperature Doppler width of an individual rotational line in the CO angstrom bands at 5198 Å is 0.012 Å.

Collins and co-workers have used a tunable dye laser with a few angstrom bandwidth to measure the attenuation or amplification for several bands of the N_2^+ first negative system (Ref. 17). However, with the much smaller bandwidth reported by Hänsch, it will be possible to measure the absorption of individual rotational lines. This will provide accurate data on the number density of excited states, and will yield a larger change for a given set of experimental conditions. Measurement of the absorption for several different rotational lines will permit determination of the rotational temperature, which will yield a much more accurate estimate of the total population of the vibrational level of a specific electronic state.

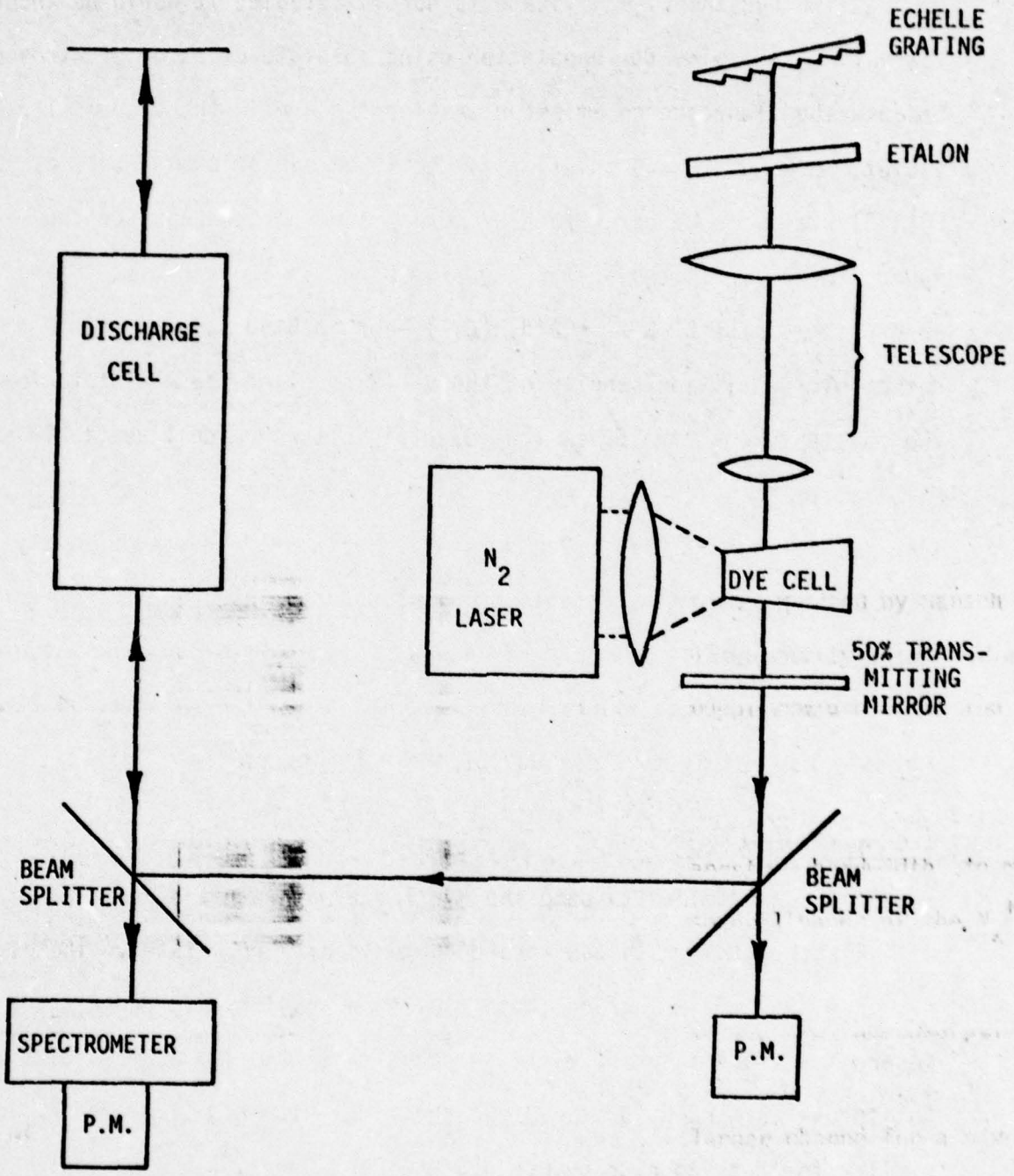

Figure 14. Block Diagram of Tunable Dye Laser Absorption Technique for Measuring Excited Electronic State Populations

Although the CO(A'Π) state is not metastable, it would be inconvenient to determine its population using absolute emission spectroscopy because the fluorescence emission wavelengths are in the vacuum ultraviolet. However, the population of the lower vibrational levels of the CO(A'Π) state can be determined by absorption spectroscopy for the appropriate transitions of the angstrom bands in the visible. Using absorption of the CO($B'\Sigma^+ \leftarrow A'\Pi$) (0,2) band at 5198 Å, the minimum detectable population density of the v = 2 level of the A'Π state for two passes through the 50-cm long electric discharge cell available at MSNW is approximately 10^{11} molecules/cm^3. The minimum detectable population densities for the v = 0 and v = 1 levels would be approximately the same. These minimum detectable population densities are lower than the values typical of visible and UV lasers produced by e-beam excitation or high-voltage electric discharge excitation. Thus the method will be directly applicable to the study of the kinetics of these lasers.

Nitrogen Pump Laser

It was decided to pump the dye laser with a nitrogen laser at 3371 Å rather than with the second harmonic of a ruby laser. The nitrogen laser has the advantage that it will be available for gain and absorption studies on the nitrogen second positive system in addition to its use as a pump for the dye laser. The nitrogen laser design is similar to that reported by Cubeddu and Curry (Ref. 18). A water capacitor connected directly to the electrodes of the gas discharge tube provides rapid transfer of the electrical energy to the gas without resorting to a large number of coaxial cables. The electrical energy is

stored in a 0.1 μf capacitor charged to 30 kV and is transferred to the water capacitor through a parallel plate transmission line utilizing a triggered spark gap as a switch.

At a nitrogen pressure of 20 torr, the laser output energy with no mirrors was roughly 5 mJ. The output energy could be increased by adding a flat mirror to one end of the cavity. Because of severe noise problems when the spark gap is triggered, the pulse duration has not been measured. The entire device is being enclosed in an aluminum box in an effort to reduce this noise problem.

Laser action has also been observed for the (0,0), (1,0), and (2,1) bands of the nitrogen first positive system when a cavity formed from gold coated mirrors is employed. Thus this laser can also be utilized as a probe for the $N_2(A^3\Sigma_u^+)$ state.

All of the components for the dye laser have been specified except the etalon, and all have been received. However, the dye laser has not been assembled or tested.

SECTION V

LASER CAVITY STUDIES

5.1. Nitrogen Second Positive System

A high-Q optical cavity was used with the 50-cm path, 5-tube plasma diode e-beam stabilized electric discharge facility to investigate the possibility of long pulse laser emission from the nitrogen $C^3\Pi_u \rightarrow B^3\Pi_g$ transition. The optical cavity consisted of dielectric coated mirrors having a 2-meter radius of curvature and spaced 1 meter apart. The mirrors were mounted internally in order to reduce the transmission losses associated with Brewster angle windows. The mirror coating has maximum reflectivity at 337 nm and provides a reflectivity greater than 99 percent over the range from 315 nm to 355 nm. This range includes the (0,0) and (0,1) bands of the nitrogen second positive system, which have wavelengths of 337.0 and 357.6 nm, respectively. However, the reflectivity at 357.6 nm has fallen to approximately 99 percent so that the mirror coating has about 1 percent transmission at this wavelength.

In addition to searching for lasing on the C → B (0,0) and (0,1) bands, we monitored the fluorescence from the (0,2) and (0,3) bands at 380.4 and 405.8 nm, respectively. Both 5:1 and 10:1 $Ar+N_2$ mixtures at 400 torr total pressure were investigated. Discharge currents of 22 A/cm^2 and values of E/N equal to 1.5 and 0.9 x 10^{-16} $V\text{-}cm^2$, respectively, were achieved for time durations of 2 to 3 μsec for the 5:1 and 10:1 $Ar+N_2$

mixtures. These values of E/N represent the maximum discharge voltage that could be applied to the gas without incurring an arc during the pumping phase. However, little or no contribution to the C state emission was produced by the discharge.

In order for the discharge to contribute to the nitrogen C state fluorescence it was necessary to either reduce the N_2 concentration or add small amounts of SF_6. When the N_2 concentration was reduced to approximately 3 percent, the nitrogen second positive emission produced by the discharge became more intense than that produced by the e-beam. This effect was observed at 400 torr total pressure with a discharge current density of 22 A/cm^2 and an E/N = 0.6 x 10^{-16}V-cm^2. The addition of approximately 0.1 percent SF_6 to the 5:1 Ar+N_2 mixture permitted a higher value of E/N, 2 x 10^{-16}V-cm^2, to be applied, which appreciably enhanced the C state emission produced by the discharge, even though the discharge current decreased by an order of magnitude. The enhancement of the nitrogen second positive emission when small concentrations of SF_6 are added to the gas mixture was discussed in the previous section for long duration pulses (10 μsec). The fluorescence emission pulse shape observed under the present conditions (2 μsec discharge pulse length and low N_2 concentration or addition of small concentrations of SF_6) followed the discharge current quite closely with no apparent contribution from the $N_2(A)$ state pooling reaction and is most likely produced by direct electron impact with ground state N_2 or by excitation transfer from excited Ar. The short pulse behavior is in contrast to that previously observed with longer discharge pulses and higher N_2 concentrations, where self collisions

of metastable $N_2(A)$ to produce $N_2(C)$ contributed significantly to the observed emission (as noted previously).

Cavity tests were also conducted at a total pressure of 700 torr for both $Ar+N_2$ and $Ar+N_2+SF_6$ mixtures. It was thought that at this pressure, the $N_2(B)$ state is collisionally deactivated by Ar in a time that is less than the $N_2(C)$ state radiative lifetime (Ref. 3), thus satisfying one of the conditions for a long pulse laser. However, the time history of the fluorescence emission was similar to that observed at 400 torr total pressure and no laser emission was observed. Subsequent studies by other groups (Ref. 8) indicate that the rate coefficient reported in Reference 3 applies only to higher vibrational levels of the $N_2(B^3\Pi_g)$ state. If the slower rate coefficients reported by the SRI group are correct, the $N_2(B)$ state would not have been collisionally deactivated more rapidly than the $N_2(C)$ state radiative lifetime under the conditions of our experiment.

5.2. Carbon Monoxide Angstrom Bands

A similar set of experiments was carried out for the $CO(B'\Sigma^+ \rightarrow A'\Pi)$ transition for quite an extensive range of conditions. The internal mirrors were dielectric coated for maximum reflectivity at 558 nm. One was coated to have a broad band reflectivity greater than 99 percent from 485 nm to 620 nm, while the other was coated to have 1 percent transmission and at least 98 percent refectivity from 520 nm to 610 nm. This wavelength range includes the (0,2), (0,3), and (0,4) bands of the CO ($B \rightarrow A$) transition with wavelengths of 519.8 nm, 561.0 nm, and 608.0 nm, respectively.

Gas mixtures containing 1 percent to 10 percent CO with He as a buffer gas were investigated at total pressures from 50 torr to 700 torr. A peak discharge current of 6 A/cm^2 at an E/N of 2.5 x 10^{-16}V-cm^2 was achieved for He + 10 percent CO mixtures at total pressures of 100 and 200 torr. Initially it was thought that laser emission was observed at 519.8 nm and 561.0 nm because the output signals at these wavelengths were observed to increase by a factor of 10 when the optical cavity was aligned. Typical oscilloscope traces showing this effect are presented in Figure 15. Subsequently, it was discovered that this enhancement was due to ordinary fluorescence being enhanced by multiple reflections within the cavity at the specific wavelengths for which the cavity was high-Q and low output coupling. This was demonstrated by adding Ar to the gas mixture and obtaining the same enchancement for an Ar line at 549.6 nm.

In addition to searching for laser action on the (0,2), (0,3), and (0,4) transitions of the CO angstrom bands, we monitored the fluorescence emission for these transitions as well as for the (0,0) and (0,1) bands. Direct excitation was predominant, with no indication of any secondary excitation process. Fluorescence emission from the (0,2) band of the CO($B'\Sigma^+ \rightarrow A'\Pi$) transition for a He + 10 percent CO mixture at 200 torr is shown in Figure 16. The discharge current is approximately 5 A/cm^2 at an E/N = 2.5 x 10^{-16}V-cm^2. The time history of the fluorescence emission essentially follows the discharge current, which implies that the CO($B'\Sigma^+$) state is lost as rapidly as it is produced. Therefore, in order to produce a larger population in this state, the pumping rate, not

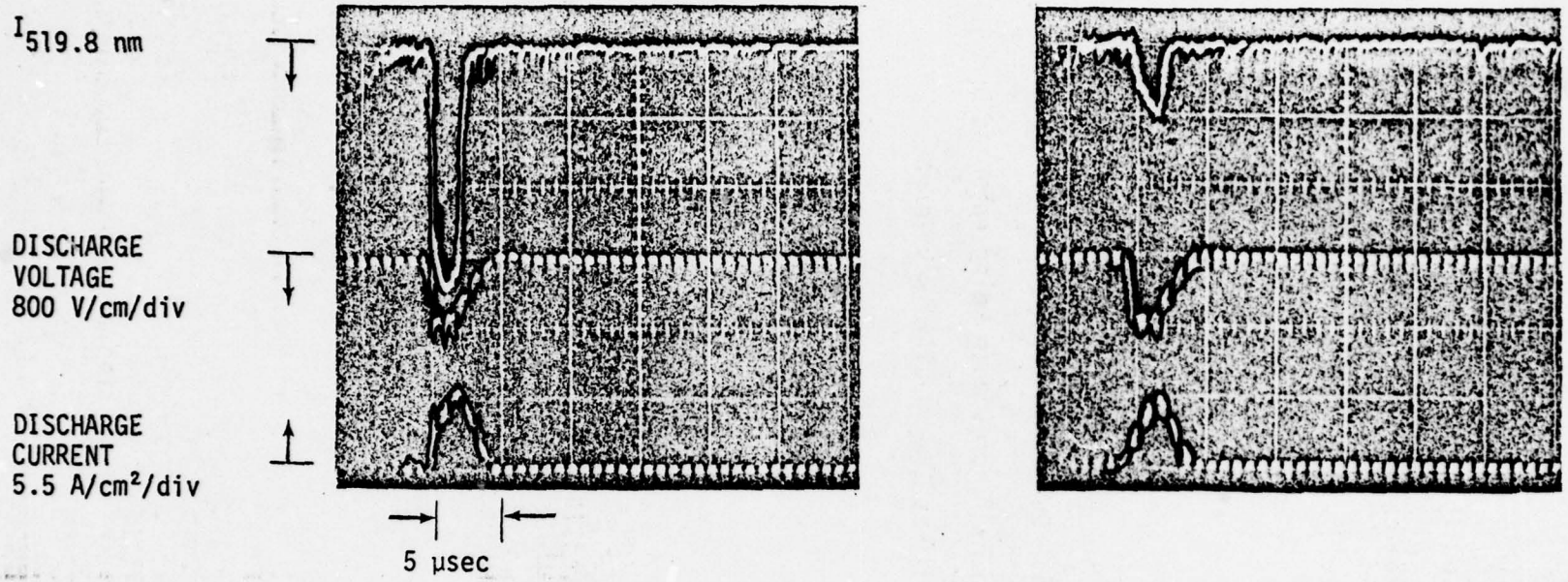

Figure 15. Cavity Intensity for the (0,2) Band of the CO($B^1\Sigma^+ \rightarrow A^1\Pi$) Transition at 519.8 nm in a He + 10% CO Mixture at 100 Torr.

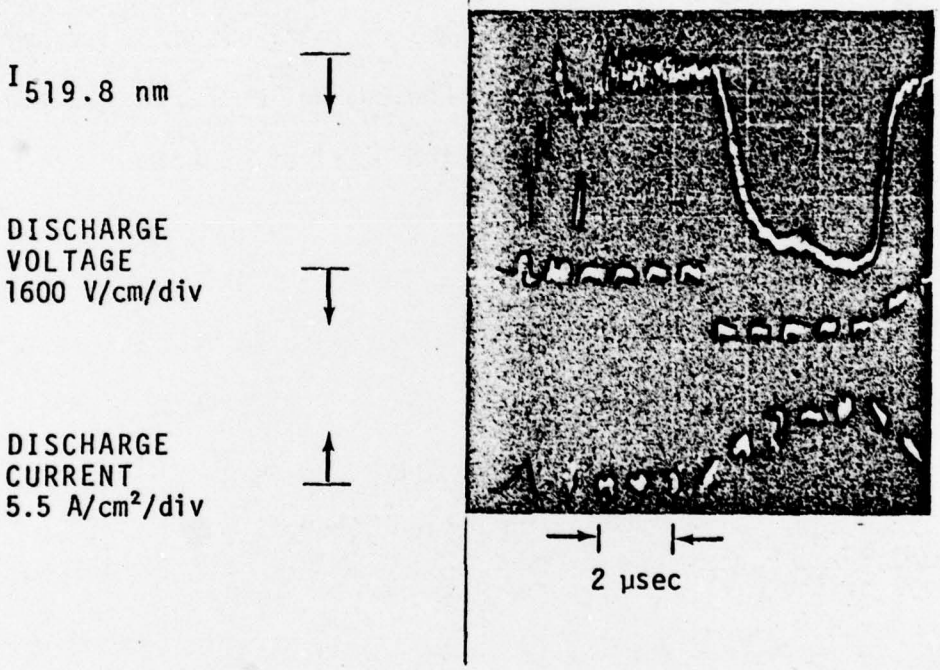

Figure 16. Fluorescence Emission from the (0,2) Band of the $CO(B^1\Sigma^+ \rightarrow A^1\Pi)$ Transition for a He + 10% CO Mixture at 200 Torr

the pumping time, will have to be increased substantially. This can be accomplished by increasing the electron density, or probably more efficiently by increasing the average electron energy.

5.3. Nitrogen First Positive System

The principal barrier to the attainment of a higher electron energy in these experiments has been the onset of arc formation if higher discharge voltages are applied. The rise time of the discharge current is of the order of 1 to 2 μsec and the total discharge pulse length was from 3 to 5 μsec. Recently, Newman, De Temple, and Coleman (Ref. 19) have reported laser action in the N_2 first positive system using a short duration, fast rise time, electron beam controlled discharge. Since previous work on the N_2 first positive system laser and the CO angstrom band laser indicates that these lasers operate under similar conditions (Ref. 20), it was decided to install a fast rise time, short duration, electric discharge power supply on the 5-tube plasma diode device. If CO could be lased in this device, then it would be possible to test some of the collisional mechanisms for achieving a long pulse laser that were described previously in this report.

The new electric discharge power supply consists of a 0.1 μf capacitor switched by a triggered spark gap. The capacitor and spark gap were connected directly to the electric discharge anode by ten pieces of RG-8/U cable that were each 3 feet long. This combination supplied a discharge current pulse with a rise time of approximately 0.1 μsec and a duration of about 1 μsec. The charging power supply limited the capacitor voltage to 25 kV corresponding to a stored energy of about 30J.

Using this power supply, laser action was observed in the N_2 first positive system at 1.05 μm (0,0) and at 888 nm (1,0). The gas mixture was pure N_2 at 70 torr total pressure. The discharge chamber was fitted with CaF_2 windows at Brewster's angle and the cavity was formed by two gold coated mirrors having a 2 meter radius of curvature and spaced 1.3 meters apart. Although severe noise generated by the triggered spark gap prevented a measurement of the discharge voltage and current, laser action was observed when the capacitor was charged to 15 kV, but not when it was charged to 10 kV. The effect of blocking the mirror farthest away from the detector on the (0,0) laser signal is shown in Figure 17. Laser action was also observed for 5:1 Ar+N_2 and He+N_2 gas mixtures at 250 torr total pressure and a capacitor voltage of 25 kV. Adding small amounts of SF_6 to the Ar + 17% N_2 mixture at 250 torr did not prevent the laser action on the (0,0) band until the SF_6 concentration approached 0.1 percent. When the SF_6 fraction reached this value, laser action no longer occurred. A summary of the gas mixtures and corresponding bands for which laser action was observed is presented in Table II.

A similar search was made for laser action on the CO angstrom bands in the visible and the nitrogen second positive system in the near ultraviolet. Using the appropriate mirrors that were described earlier, tests were carried out for a wide range of gas mixtures, total pressures, and applied voltages with cavities having both external and internal mirrors. No laser emission was observed in any of these experiments. This is probably due to the fact that the pumping rate is not yet high enough for these systems. Since for constant gain the

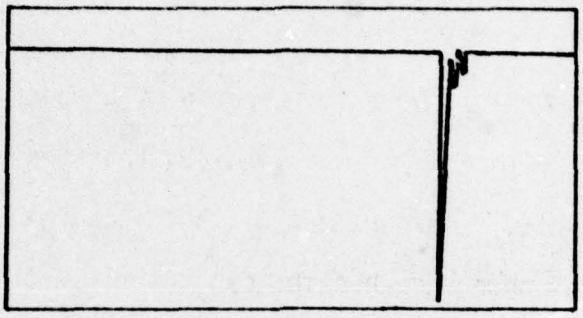

CAVITY

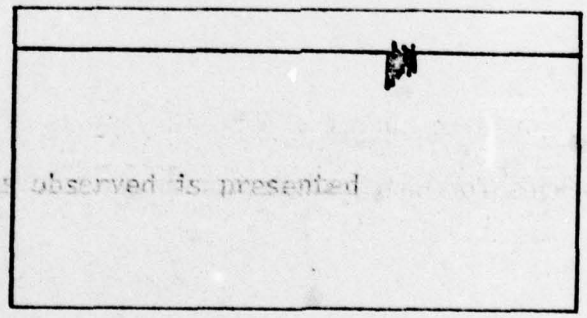

CAVITY BLOCKED

Figure 17. Oscilloscope Trace of the Cavity Intensity for the (0,0) Band of the $N_2(B^3\Pi_g \rightarrow A^3\Sigma_u^+)$ Transition in Pure N_2 at 70 Torr

Table II

$N_2(B^3\Pi_g \rightarrow A^3\Sigma_u^+)$ Electronic States Laser Transitions
Produced with E-Beam Stabilized Discharge

Wavelength (μm)	Band	Gas Mixture	Pressure (torr)
1.047	(0,0)	N_2	70
		Ar + 16% N_2	250
		He + 16% N_2	250
		Ar + 16% N_2 + 0.1% SF_6	250
0.888	(1,0)	N_2	70
		He + 16% N_2	250

molecular pumping rate scales as λ^{-3} (Ref. 21), the CO angstrom bands would require approximately an 8 times higher pumping rate and the N_2 second positive system approximately a 30 times higher pumping rate than is necessary for the N_2 first positive system. However, in order to assess with certainty why laser action was not observed in these systems, it is necessary to measure the populations of the electronic states of interest. The development of techniques to measure these populations and preliminary results of absorption measurements on the $N_2(A^3\Sigma_u^+)$ state are described in the previous section.

SECTION VI

CONCLUSIONS AND RECOMMENDATIONS

A feasible collisional mechanism has been formulated as a basis for efficient, long pulse visible lasers operating on excited electronic states of diatomic molecules. Experimental studies of electron-beam-stabilized electric discharge excitation of N_2 and CO showed two major difficulties: Considerable vibrational excitation along with electronic excitation, and arc breakdown restrictions on the E/N that could be sustained. By utilizing a short duration, high voltage e-beam stabilized electric discharge, laser action has been observed in the N_2 first positive system in the near infrared. However, similar experiments did not produce lasing in the CO angstrom bands or the N_2 second positive system. It is concluded that visible lasers to be operated on high lying electronic states will require high E/N, high power density excitation with accompanying arc breakdown restrictions. These lasers may be more amenable to excitation from above (e.g., by electron-ion recombination during e-beam ionization) rather than from below by electron impact excitation. In order to develop efficient collisional lasers on molecular electronic states excited by e-beam stabilized electric discharges, it will be advantageous to utilize molecules with suitable low-lying electronic states.

A knowledge of the population of specific excited electronic states is necessary in order to evaluate the kinetic processes taking place in electrically excited gas laser mixtures. A probe laser

absorption technique has been applied to $Ar+N_2$ gas mixtures to determine the populations of the v = 0 and v = 1 levels of the $N_2(A^3\Sigma_u^+)$ state. A more general absorption technique utilizing a narrow bandwidth, tunable dye laser has been devised for application to the $CO(A'\Pi)$ state or to other molecules having transitions in the visible. Absolute spectral emission techniques should be combined with the absorption techniques in order to provide direct measurements of the populations of the vibrational levels of the electronically excited states of candidate laser molecules.

REFERENCES

1. S. R. Byron, L. Y. Nelson, C. H. Fisher, G. J. Mullaney, and A. L. Pindroh, Final Report, Molecular Lasers in E-Beam Stabilized Discharges, MSNW Report No. 75-105-4, February 1975.

2. J. W. Dreyer and D. Perner, J. Chem. Phys. 58, 1195 (1973).

3. R. A. Young, G. Black, and T. G. Slanger, J. Chem. Phys. 50, 303 (1969).

4. P. Millet, Y. Salamero, H. Brunet, J. Galy, D. Blanc, and J. L. Teyssier, J. Chem. Phys. 58, 5839 (1973).

5. J. W. Dreyer and D. Perner, Chem. Phys. Lett. 16, 169 (1972).

6. F. J. Comes and E. H. Fink, Z. Naturforsch. 28a, 717 (1973).

7. E. H. Fink and F. J. Comes, Chem. Phys. Lett. 25, 190 (1974).

8. R. M. Hill, R. A. Gutcheck, D. L. Huestis, D. Mukherjee, and D. C. Lorents, Technical Report No. 3, Studies of E-Beam Pumped Molecular Lasers, SRI Report No. MP 74-39, July 1974.

9. G. N. Hays and H. J. Oskam, J. Chem. Phys. 59, 6088 (1973).

10. D. W. Setser, D. H. Stedman, and J. A. Coxon, J. Chem. Phys. 53, 1004 (1970).

11. T. Kasuya and D. R. Lide, Jr., Appl. Opt. 6, 69 (1967).

12. D. E. Shemansky and A. L. Broadfoot, J. Quant. Spectrosc. Radiat. Transfer 11, 1385 (1971).

13. A. Schadee, Bull. Astr. Inst. Neth. 17, 311 (1964).

14. A. Budó, Z. Physik 96, 219 (1935).

15. G. N. Hays and H. J. Oskam, J. Chem. Phys. 59, 1507 (1973).

16. T. W. Hänsch, Appl. Opt. 11, 895 (1972).

17. C. B. Collins, A. J. Cunningham, S. M. Curry, B. W. Johnson, and M. Stockton, Appl. Phys. Lett. 24, 245 (1974).

18. R. Cubeddu and S. M. Curry, IEEE J. Quant. Electron. QE-9, 499 (1973).

19. L. Newman, T. A. De Temple and P. D. Coleman, paper MA4, "N_2 Infrared Laser Operation in an Electron Beam Controlled Discharge" presented at the 4th Conference on Chemical and Molecular Lasers, St. Louis, Missouri, October 21-22, 1974.

20. P. K. Cheo and H. G. Cooper, Appl. Phys. Lett. 5, 42 (1964).

21. C. K. Rhodes, IEEE J. Quant. Electron. QE-10, 153 (1974).